Available online at www.sciencedirect.com

ScienceDirect

Current Opinion in
Colloid & Interface Science

Active colloids on fluid interfaces

Jiayi Deng[1], Mehdi Molaei[2], Nicholas G. Chisholm[3], Tianyi Yao[1], Alismari Read[1] and Kathleen J. Stebe[1]

Abstract

We review recent work on active colloids at interfaces, including self-propelled colloids that move by generating a propulsive force, and driven colloids that move under external fields. Features unique to fluid interfaces alter the flows generated at interfaces by active colloid motion, and hydrodynamic interactions with these layers. We emphasize recent observations of natural swimmers, like bacteria, and biomimetic colloids including self-propelled phoretic and Marangoni swimmers, and magnetically driven colloids. We discuss active colloid interaction with boundaries and with each other. We conclude with a discussion of open issues and opportunities to design active colloids as active surface agents that manipulate interfacial properties and the transport in the vicinity of interfaces.

Addresses

[1] Department of Chemical and Biomolecular Engineering, University of Pennsylvania, Philadelphia, PA, USA
[2] Pritzker School of Molecular Engineering, University of Chicago, Chicago, IL, USA
[3] Mathematical Sciences, Worcester Polytechnic Institute, Worcester, MA, USA

Corresponding author: Stebe, Kathleen J. (kstebe@seas.upenn.edu)

Current Opinion in Colloid & Interface Science 2022, **61**:101629

This review comes from a themed issue on **Special Topic Volume: Active Colloids (2022)**

Edited by **Marie Pierre Krafft**, **Orlin D. Velev** and **Nicholas Lawrence Abbott**

For complete overview about the section, refer Special Topic Volume: Active Colloids (2022)

https://doi.org/10.1016/j.cocis.2022.101629

Keywords

Active colloids, Fluid interfaces.

Introduction

We review aspects of recent research on active colloids, including driven colloidal particles that move under the action of external fields, and swimmers or self-propelled colloidal particles. Driven colloidal particles serve as probes to report on the local properties of their milieu [1–4] and are used as building blocks in directed assembly schemes for functional structures [5–8]. Active colloids are widely studied for insight into biology and into physics of far-from-equilibrium structures. For example, bacteria have been widely studied as self-propelled microscale swimmers to understand their implications in nature including bacterial locomotion, surface attachment, quorum sensing, colony formation and biofilm development [9–14]. In addition to providing insight into microbial biology, bacteria's persistent and efficient swimming and their ability to self-organize are studied for fundamental insight into collective dynamics and to guide the design of biomimetic swimmers [15–18]. The hydrodynamics of active colloids in isolation, the nature of their hydrodynamic interactions, and other physico–chemical interactions with their milieu and with confining boundaries are widely studied to understand their ability to orient, trap and organize. These diverse responses are harnessed in application as "physical intelligence" in micro-robotic schemes that allow active colloids to sense and respond to their surroundings [19].

Active colloids accumulate at fluid interfaces, where they can either move adjacent to the interface or adsorb and move on the interface itself. This active adsorbed state is unique to fluid interfaces, as particles adsorbed on solid boundaries typically cannot translate. Active colloid association with fluid interfaces provides new opportunities to design system response. Interfaces between two immiscible fluids are not only sites where the viscosity changes rapidly from that of one bulk phase to another. Rather, they are highly anisotropic environments with complex physics and chemistry. Interfaces are open systems, in contact with the two adjacent bulk phases. Furthermore, interfaces have elevated surface energies or surface tensions that promote adsorption and accumulation of material from either phase. Classically, small molecule surfactants, surface active macromolecules, and passive colloidal particles are assembled at interfaces to stabilize dispersions and impart functionality. More recently, droplets stabilized and propelled by active colloids have been studied, with exciting implications for droplet motion and for local mixing near the interface.

There are excellent recent reviews on active colloids and interfaces, indicating the strong interest in this field [20,21]. Since we have been studying active colloids at interfaces to understand their motion and the flows that they generate [22,23], we focus on the literature in

these arenas. This review is divided into five parts, of which this Introduction is the first. In the second part, we describe background regarding the manner in which interfaces constrain particles or alter their motion. In the third section, we highlight the propulsion of active colloids at interfaces via diverse mechanisms, including natural swimmers, biomimetic self-propelled colloids, and driven colloids. In the fourth part, we discuss active colloid interaction and application. Finally, we conclude this review with a discussion of opportunities for the future study.

Background

Active colloids with radius a, moving at velocity U near or on an interface between fluids of mean density $\bar{\rho}$ and mean viscosity $\bar{\mu}$ typically move with Reynolds number $\mathrm{Re} = \bar{\rho}Ua/\bar{\mu} \ll 1$, so inertial effects can be neglected. The importance of gravitational effects depends on the Bond number $Bo = \Delta\rho g a^2/\gamma$ where g is gravitation acceleration, and $\Delta\rho$ is the difference in density between the particle and the subphase; for colloidal scale particles, gravitational effects are often negligible. Active colloids typically move in a regime of negligible capillary number $Ca = \bar{\mu}U/\gamma$, which characterizes the ratio of viscous stresses to surface tension γ, so active particle motion cannot deform the fluid interface. Colloid motion is resisted by drag force F_D characterized by a drag coefficient $C_D = F_D/\bar{\mu}Ua$ that is influenced by the degree of immersion of the colloid in the bulk fluids, and the stresses in the interface. For adsorbed colloids, the behavior of the contact line plays an important role in constraining particle motion. In this section, we review fundamental concepts important for understanding the motion of active colloids. We then discuss stresses at fluid interfaces and their implications for active colloid motion.

Particle adsorption and contact-line pinning

A passive spherical particle with negligible weight attached to a fluid interface has a contact line where the interface intersects the particle. At equilibrium, adsorbed colloidal particles are typically trapped as their presence at the interface lowers the net surface energy of the system by as much as 10^5 k_BT [24]. Young's equation predicts that the interface will adopt an equilibrium contact angle at the contact line, thereby defining a unique adsorbed configuration for the particle at equilibrium. However, a recent body of research has shown that contact lines display complex dynamics that depend on the particle's surface composition and nanoscale topography, even for particles with ostensibly uniform surface chemistry. When attaching to an interface, a colloid first breaches interface, forming a contact line and releasing capillary energy; thereafter, the contact line evolves towards equilibrium [25–29]. Contact lines can evolve with glassy dynamics during which its location evolves logarithmically in time [27]. This evolution is consistent with contact line pinning to nanoscopic heterogeneities with characteristic hopping frequencies between pinning sites as the system tends to equilibrium [30].

Contact line dynamics have been studied for diverse particle materials, surface chemistries, particle sizes, for particles approaching interfaces from aqueous and oil phases [28]. For most particles studied, after initial dynamics associated with breaching subsided, contact lines evolved with glassy dynamics, thereafter crossing over into a rapid relaxation regime. The duration of glassy dynamics was highly dependent on the particle material. Simulation captures three distinct regimes of contact line relaxation [29], including an initial exponential decay associated with visco-capillary dynamics, which crossed over to slow logarithmic relaxation, followed by a final exponential decay close to equilibrium. These studies address contact line pinning on relatively smooth spherical colloids. However, many active colloids are highly heterogeneous or patchy, with complex surface topographies and surface chemistries, known to generate even more complex contact line pinning effects [31]. Pinning and variations of the contact line height generate long-ranged capillary interactions between particle pairs [32] and between the particles and the underlying interface curvature [33].

If present, contact line pinning would have important implications for adsorbed active colloids. For example, pinned contact lines would trap active colloids with similar features in widely different surface configurations. Such diverse configurations have been reported for bacteria swimming in an adsorbed state on oil–water interfaces [22]. Contact line pinning would constrain colloidal motion, disallowing rotation about axes in the plane of the interface. The persistence of diverse trapping states would imply that differing flow fields would be generated around the particles, as the active particle's configuration influences the degree of immersion and the flow generated in the adjacent fluids, all of which should alter the flow in the interface. The resulting drag resisting active colloid motion would also be influenced by contact line dynamics. Locomotion can also depend on the adsorbed colloid's configuration, for either driven or self-propelled particles. For example, colloids driven by external electric fields can be anticipated to respond differently depending on their degree of immersion at interfaces between fluids with different dielectric properties or ion concentrations. Bacteria motion depends on the immersion of flagella in an aqueous phase, and catalytical active patches require access to the chemicals typically presented in aqueous phases to fuel their motion.

Stresses in fluid interfaces

Surface-active molecules adsorb at fluid interfaces and lower the surface tension. These adsorbed molecules can be redistributed by the flow around active colloids,

generating complex stress responses that alter active colloid motion. For a comprehensive review of these effects, see the study by Manikantan et al. [34]. Here, we give a brief overview to note important limits that are encountered in experiment. For isothermal systems, the surface tension γ depends on the surface concentration of surfactant Γ via a surface equation of state $\gamma(\Gamma)$. The stress balance at a fluid interface requires that the jump in the normal stress be balanced by the product of the mean curvature of the interface and interfacial tension, as well as any normal stresses from surface rheology including dilatational viscous stresses and elastic responses. Tangential stress discontinuities are balanced by surface tension gradients or Marangoni stresses and tangential stresses arising from the surface rheology.

Dimensional analysis of the stress balance yields two dimensionless numbers, the first being the Marangoni number $Ma = \left(- \left(\frac{\partial \gamma}{\partial \Gamma}\right)_{\Gamma=\Gamma_c} \Gamma_c \right) \Big/ \bar{\mu} U$, where the Marangoni stress has been expressed via a chain rule in terms of derivatives of the equation of state $\left(\frac{\partial \gamma}{\partial \Gamma}\right)_{\Gamma=\Gamma_c}$ evaluated at a characteristic surface concentration Γ_c. This number characterizes the ratio of Marangoni stresses to viscous stresses exerted on the interface. The second dimensionless number is the Boussinesq number $Bq = \mu_s/\bar{\mu} a$, which characterizes the importance of dissipation by surface viscous to bulk viscous effects. We focus first on Marangoni stresses, which can often dominate the stress state of the interface for small molecule surfactants. The distribution of surfactant on the interface Γ is determined by the surface mass balance, which can be stated in dimensionless form as:

$$\frac{\partial \Gamma'}{\partial t'} + \nabla'_s \cdot \left(\boldsymbol{u}'_s \Gamma'\right) - \frac{1}{Pe_s} \nabla'^2_{\mathbf{s}} \Gamma' = -j'_n \qquad (1)$$

where, a/U is used as the characteristic timescale. In this expression, $\nabla'_s \cdot (\boldsymbol{u}'_s \Gamma')$ captures surface convective effects including tangential advection and interfacial dilatation, and $\nabla'^2_{\mathbf{s}} \Gamma'$ represents the surface diffusive effects. The normal flux from the bulk j'_n captures the exchange of surfactant between the bulk and the interface.

The surface Peclet number $Pe_s = aU/D_s$ characterizes the ratio of convective to diffusive transport of the surfactant at the interface, where D_s is the surface diffusivity. Pe_s is typically large, so surface diffusive fluxes are typically weak. For an active colloid moving in an otherwise uniform surfactant covered interface, convection in the interface generates surface concentration gradients, and mass transfer between bulk phases and the interface relieves these gradients. Thus, the magnitude of j'_n plays an essential role in determining interfacial stress response. We describe two regimes, $j'_n \ll 1$ and finite j'_n, below.

Insoluble surfactants or very slow surfactant exchange between the interface and the bulk phase: The flux from the bulk, j'_n can be negligible for sparingly soluble surfactants or for dilute surfactant solutions which have slow exchange with the interface. If either bulk phase is very viscous, Ma approaches zero, and Marangoni stresses are negligible. In this limit, the interface acts only as a constant surface tension dividing surface in the flow. Recently, Dani et al. [35] reported drag on particles at interfaces that obey this limit for heavy Teflon particles trapped at highly viscous polyalphaolefin oils interfaces. If, however, surfactant is dilute and the adjacent fluids have viscosities comparable to that of water, $Ma = \frac{RT\Gamma_c}{\bar{\mu} U} \gg 1$. In this regime, large Marangoni stresses drive gradients in Γ to zero. The steady surface mass balance becomes $\nabla'_{\mathbf{s}} \cdot \boldsymbol{u}'_s = 0$, which requires that the interface behaves as an incompressible layer [36–38]. In this limit, the drag [38], mobility [37], interfacial Stokelet and image forces [39] have been found for particles moving on or near incompressible interfaces. Recently, higher order hydrodynamic multipoles for driven and active colloids near or on clean or incompressible interfaces have be derived [40]. A flow field consistent with this limit has been observed in experiment around thermal particles at aqueous–air interfaces [41], shown in Figure 1a. Importantly, this limiting behavior will be typically encountered in studies of active colloids at interfaces with ostensibly "clean" or surfactant-free interfaces.

Finite exchange between the interface and the bulk phase: Generally, for soluble surfactants, the surface concentration in a quiescent system is determined by the equilibrium adsorption isotherm $\Gamma(C)$ where C is the bulk surfactant concentration. Around a moving adsorbed colloid, the bulk field C is determined by a balance of convection and diffusion, and fluxes between the bulk fluid and the interface are determined by the serial processes of diffusion from solution toward the interface and the kinetics of adsorption–desorption exchange. When these rates of exchange are finite compared to the convective time scales, j'_n must be formulated in terms of diffusive fluxes and adsorption–desorption fluxes, and the effective stresses in the interface are determined for finite Ma by the simultaneous solution of the stress balance, bulk and surface mass balances, and flow field. Furthermore, outside of a surface gaseous regime, the surface equation of state is non-linear. These fully coupled regimes remain areas of active research [42].

Flow in the interface

Flow induced by colloidal motion near interfaces can be understood through far-field analyses that give the universal flow characteristics that prevail sufficiently far from an active colloid but neglect near-field details, and detailed simulations that account for colloid geometry and propulsion mechanisms, allowing one to construct accurate near-field flow fields or to predict specific

Figure 1

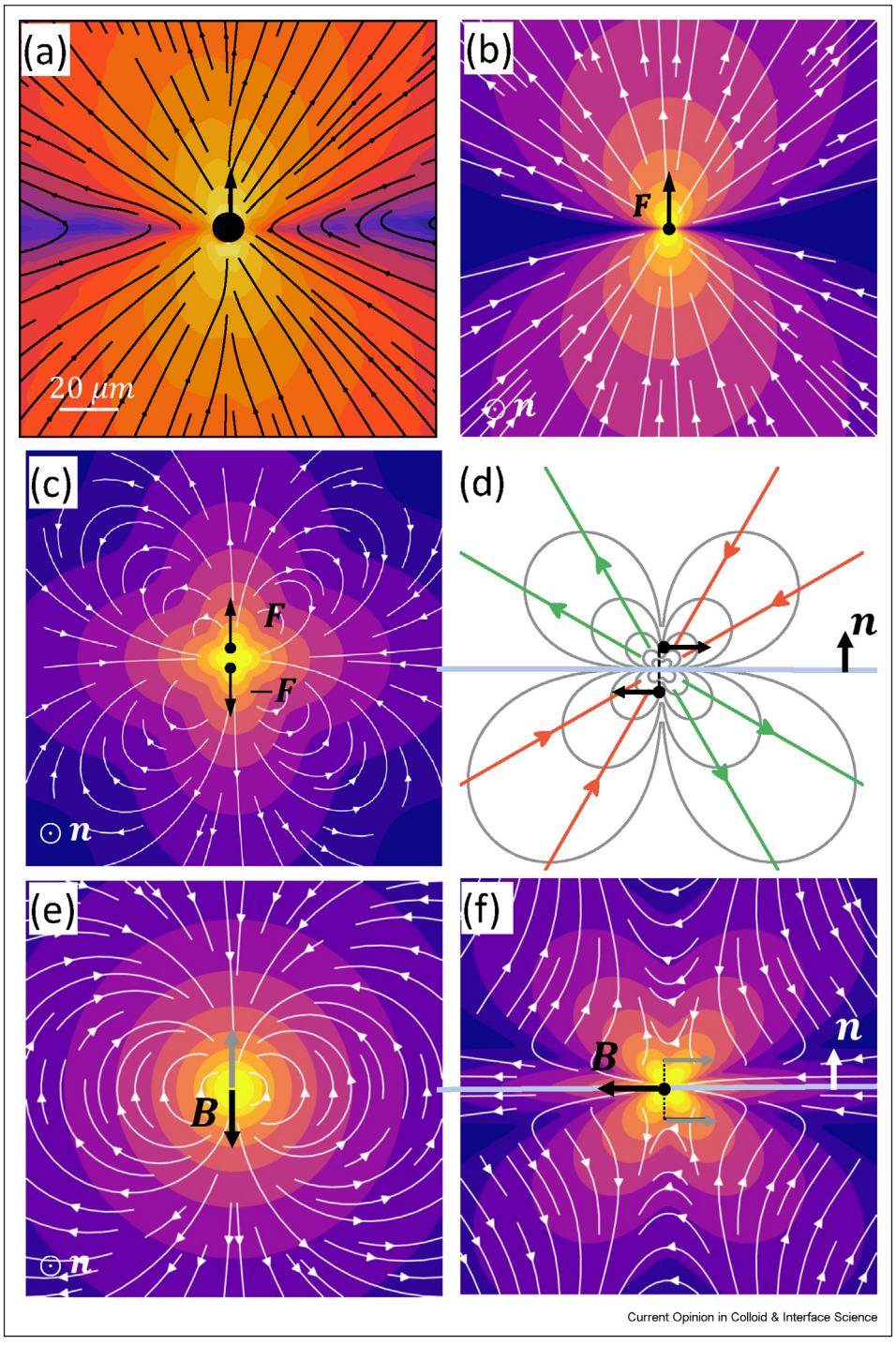

Hydrodynamic multipoles for incompressible interfaces. (**a**) Interfacial Stokeslet measured experimentally from Brownian particles (Adapted from the study by Molaei et al. [41]) and its theoretical predictions shown in (**b**). (**c**) Top view of an incompressible stresslet. (**d**) Side view of asymmetric mode. (**e**) Interfacial flow of off-interface forcing mode and its side view shown in (**f**). (Adapted from the study by Chisholm et al. [40]).

colloid trajectories [43–45]. Far-field hydrodynamic models have been surprisingly useful in understanding the behaviors and interactions of colloids. The leading-order far-field flow of colloids driven by an external force can be described as a simple point force on the fluid at the location of the colloid in an otherwise quiescent fluid; the flow field, which decays with distance r from the colloid as $1/r$ is termed a "Stokeslet".

Similarly, colloids driven by an external torque can be described by a point-torque or "rotlet", which decays as $1/r^2$. These modes universally describe flows far from driven objects. However, they do not capture the details of flows very close to the driven colloids that depend on their shape or surface features. To capture such effects, higher order modes (torque dipoles, quadrupoles, octupoles) or detailed simulations are required.

For self-propelled objects, however, the leading-order flow is given by a force dipole, reflecting the lack of a net external force on the system; instead, a thrust-drag force pair is exerted on the fluid. Various higher-order modes may be ascribed to different characteristics of an active colloid. In the case of a flagellated bacterium, a torque dipole can be induced by counter-rotation of the body and flagella during locomotion; a Stokeslet quadrupole arises from length asymmetry between the flagella and the cell body; and a source-sink doublet due to the finite size of the cell body [9]. In contrast to a bulk fluid, where a multipole expansion about a single point within the colloid is sufficient to describe the flow, the abrupt change in viscosity between the fluid phases and nontrivial rheology of the interface necessitates the summation of three separate multipole expansions; one that is about a point located above, below, and exactly on the interface, with the three expansion points separated by an infinitesimal distance from a central location within the colloid of interest [40]. Here, we briefly summarize the leading-order modes for driven and active colloids moving near or on incompressible fluid interfaces. We consider colloids with pinned contact lines if they are in an adhered state on the interface. In this discussion, colloids are approximated point forces, torques and higher order stress moments exerted on the (otherwise quiescent) system about a point on the interface.

For an incompressible interface, a colloid driven by a parallel force generates a surface-incompressible force monopole, or "interfacial Stokeslet" at leading order, which features symmetry of the velocity field about the interfacial plane (Figure 1b). This flow is "lamellar"; the velocity field is directed parallel to the interface, even for points off the interfacial plane. This type of flow is a general characteristic of a fluid bounded by a planar interface that moves in an incompressible manner [46]. For a colloid forced adjacent to the interface in a direction normal to the interface, a rather weak quadrupolar flow, with a $1/r^3$ velocity decay in the bulk and no flow on the interface arises at leading order. This leading-order flow is identical to that expected for a *rigid* plane boundary with a colloid in the same configuration [36]. This differs from a clean interface, for which local interfacial expansion and contraction can occur, resulting in a viscosity-averaged stresslet, or a symmetric force dipole aligned normal to the interface. However, for a colloid adhered by contact-line pinning, a normal force exerted on the colloid is completely supported by the non-deformable interface and no force is transmitted to the fluid.

An external torque normal to the interface generates a velocity field equivalent to that of a rotlet in a bulk fluid having the average viscosity of the two fluids, $\bar{\mu} = \frac{1}{2}(\mu_1 + \mu_2)$. An external torque parallel to the interface produces no flow for adhered particles because such torque is supported by the pinned contact line instead of being transmitted to the fluid. However, an asymmetric, off-interface dipolar mode (Figure 1d) can be generated for an adjacent particle forced to rotate by a torque parallel to the interface. This mode also is associated with an unequal distribution of force exerted by the colloid on the upper and lower fluids. In contrast to the parallel interfacial Stokeslet and normal interfacial rotlet, which feature planar symmetry and only depend on the average viscosity, this asymmetric dipole exhibits a viscosity-weighted antisymmetry about the interface, where the flow exactly on the interface vanishes and the flow speed in the more viscous phase is slower by a factor of the viscosity ratio.

The interfacial Stokeslet and rotlet terms vanish for a self-propelled active colloid. For swimmers, the first surviving modes are force dipoles. On incompressible interfaces, a stresslet parallel to the interface generates flow with a four-lobed structure of closed streamlines at the interface shown in Figure 1c and lamellar flow in the adjacent phases. Because of interfacial incompressibility, forces near the interfaces are balanced by Marangoni stresses in the interface. For finite-sized swimmers with off-interface sites of propulsive force, two additional dipolar modes arise. The first is the asymmetric dipole that we have already discussed, which here is associated with an uneven distribution of thrust and/or drag between the two fluid phases. The second, a symmetric dipole which we term the off-interface forcing mode, generates a non-lamellar flow unique to incompressible fluid interfaces that is independent of viscosity contrast and symmetric with respect to the interfacial plane. It constitutes a doublet of force dipoles just above and below the interface as illustrated in Figure 1e and f. Together, they exert equal forces parallel to the interface at points just above and below the interfacial plane, and a balancing force on the interface.

In a bulk fluid or at an ideal, clean interface, such a dipole doublet induces a *quadrupolar* flow that decays as $1/r^3$, but, here, the discontinuity of tangential stress at the interface afforded by Marangoni effects cause this mode to retain a dipolar character, decaying as $1/r^2$. (The same mode also arises and contributes to the higher order flow for driven colloids that protrude into the adjacent fluids from an incompressible interface [41].) To conclude, the general leading order flow generated by an adhered active colloid on an incompressible interface is a superposition of a parallel stresslet, an asymmetric

off-interface dipole and a symmetric off-interface forcing mode.

Drag on a particle in a fluid interface

There are many recent reviews of analysis and measurement of the drag on particles moving on or near fluid interfaces [44,1,47]. We briefly review only key concepts to underscore the complexities in considering drag on active particles moving at or near interfaces. Assuming negligible surface viscoelastic effects (negligible Bq) and Marangoni stresses (negligible Ma), the drag force on a particle straddling the interface has been approximated $F_D = 6\pi\mu^* Ua$ where μ^* is the mean viscosity on the particle surface based on its degree of immersion [48]. Analysis shows that this approximation holds for particles half immersed in either fluid, but that it over predicts the drag as the particle becomes more immersed in the viscous phase by as much as 30% [49–52,35,53]. Experiments compare favorably to these predictions in the limit of negligible Ma [35]. For large Ma, absent significant exchange of surfactant between the interface and the bulk, interfaces are incompressible. Analyses show that the drag on translating particles depends strongly on interfacial incompressibility and on the surface rheology intrinsic to the interface [38]. Mobilities of particles adjacent to incompressible interfaces differ significantly from their clean interface counterparts [37].

There are open issues, even for ostensibly surfactant-free interfaces. For example, a recent study reported anomalously high drag around particles at aqueous–air interfaces whose mechanism remains a topic of debate [54]. The drag was found to be greater for particles protruding more significantly in air. To explain this unanticipated dependence, dissipation mechanisms have been proposed that rely on dynamics in the vicinity of the contact line.

Surface rheology

The theoretical framework to understand the effects of surface rheology on particle motion are well established. In a seminal analysis, Saffman and Delbrück [55] found the mobility of a flat disk embedded in a viscous, incompressible membrane separating two semi-infinite fluids in the limit of large Boussinesq number; this analysis was extended to address moderate Boussinesq numbers [56] and subphases of finite depth [57]. Later theoretical work quantified the response of a linearly viscoelastic membrane to an embedded point force [58]. The response of interface to a point force yields the surface Oseen tensor to develop analytical solution for hydrodynamic drag on objects of arbitrary shape [56,38].

Within this framework, the motion of active particles is often analyzed to probe and elucidate the origins of excess stresses conditions at fluid interfaces. For a simple viscous interface with the interfacial shear (μ_s) and dilatational viscosities (κ_s) the interfacial stress tensor is defined as

$$\boldsymbol{\tau}_{rheo} = \mu_s\left[\nabla_s \boldsymbol{v}_s + (\nabla_s \boldsymbol{v}_s)^T\right] + \kappa_s(\nabla_s \cdot \boldsymbol{v}_s) \qquad (2)$$

The importance of the interfacial shear stress with respect to the shear stresses of the subphase fluid is characterized by the hydrodynamic length scale of the interface $l_s = \frac{\mu_s}{\bar{\mu}}$.

To measure the mechanics of complex interfaces with small surface excess rheology, it is rational to use measurement probes with small effective size compared to the characteristic hydrodynamic length scale. In these settings, driven colloidal particles are particularly effective probes, exploited in the field of active microrheology, where micron size probes including ferromagnetic microbuttons [4,59] or ferromagnetic rods [60] are driven by a sinusoidal magnetic field. The amplitude of the induced displacement and its phase lag relative to the driving field are measured to determine the complex drag resistance of the particles and to characterize the complex viscosity of the interface. Rheology of many different systems including aging asphaltene layers [61], phospholipid monolayers with nonlinear chiral rheology [62], and phospholipid monolayers with fibrinogen have been investigated using this technique [63].

Another class of active inclusions in 2D systems between two bulk fluids is molecular machines in membranes. In a seminal article, Manneville et al. [64] reported the effect of transmembrane protein activity on lipid membrane fluctuation by integrating light-driven proton pumps in the bilayer of giant vesicle. Since then, the motions and conformational changes of active transmembrane proteins have been investigated to understand transport phenomena in the cellular membrane. These force- and torque-free membrane inclusions induce long-ranged hydrodynamic displacements [65]. Active proteins are shown to behave like oscillating force dipoles that generate hydrodynamic flows and enhance diffusion of passive particles [66]. Recently, Manikantan [67] has developed a theoretical framework to study the hydrodynamic interactions and clustering mechanisms of these active membrane inclusions. Such studies may lead to new and more sensitive probes for fluid interfaces in general.

We conclude by noting that it is often difficult to determine if excess stresses in the interface must be attributed to dissipation by surface viscosities or Marangoni stresses [68]. Uncertainty in the way that particle motion shears the interface further adds to this ambiguity and make deducing interfacial viscosity from either translational or rotational drag resistance of the particle

challenging. Direct visualization of the displacement of markers in the interface around interfacial probes is suggested as an effective means of confirming underlying hypothesis in models of drag resistance. For example, Zell at al. [69] measured the displacement field at the interface of dilute SDS solutions around rotating microbuttons. They observed that the angular displacement around the microbutton decays quadratically with distance as expected for the region of small Bq number subphase dominated incompressible flow. In recent research, we have developed a new method that allows some of this ambiguity to be removed, at least for interfaces with sparing amounts of surfactant. Rather than measuring the drag on particles at the interface to infer the stress state, we image the flow field in the interface. For example, we image the interfacial Stokeslet around particles moving on the interface, revealing significant differences from the Stokeslet predicted for clean interfaces. While we take pains to avoid the contamination from the surfactant, the interfacial Stokeslet flow has the form on an incompressible Stokeslet. Subtle features of the flow field, which can be understood in from higher order multipoles at incompressible interfaces, reveal effects of the surface rheology and the finite particle size. These features in the flow field allow us to identify an upper bound on the surface viscosity [41].

Swimmers at fluid interfaces

Natural swimmers

Microorganisms like bacteria and algae are important self-propelled objects that harness energy to navigate through fluid media. These self-propelled objects typically move in Stokes flow, with negligible inertia due to their small size and swimming velocities. To self-propel, they generate a propulsive force by non-reciprocal motion of their flagella that is balanced by viscous drag on their cell body. This balance determines their translational velocities. Thus, the leading-order flow field around a swimmer immersed in a bulk fluid is described by a parallel force dipole or stresslet. Bacteria swim in "pusher" modes, with their cell body forward, generating an extensile dipole, or in "puller" modes with their cell body behind their flagella, generating a contractile dipole [9]. In bulk fluids, experiment has confirmed that the parallel force dipole captures the main features of the far-field velocity around natural pushers [70] and pullers [71]. Fluid–fluid interfaces significantly impact the locomotion of these swimmers and can be anticipated to alter their induced velocity fields due to the complex physicochemical environment, including the viscosity contrast, capillary effects like interfacial trapping, contact line pinning, and interfacial stress conditions.

Bacteria near interfaces

The effect of fluid interfaces on bacterial locomotion was first observed for bacteria swimming adjacent to boundaries. The observed locomotion depends on the type of boundary and the presence of adsorbed materials at fluid interfaces. For example, while *Escherichia coli* swim along curved trajectories in clockwise (CW) motions near solid surfaces, they swim in both CW and counterclockwise (CCW) senses near a free surface [72]. The trajectories of *Caulobacter crescentus* swarmer cells moving in pusher mode depends on the interfacial chemistry [73]. Trapping and tight CCW circular swimming is reported for interfaces of air and nutrient-rich growth medium; circular swimming does not occur if the surfactant Triton-X 100 is present. Trapping is also absent at interfaces of air-minimal salt motility medium.

Pioneering studies indicate that, as a bacterium approaches the interface, its locomotion is influenced by hydrodynamic interactions amenable to analysis. Lopez and Lauga [39] considered a far-field solution in which a bacterium swims adjacent to a fluid interface. The swimmer is modeled in terms of hydrodynamic multipoles including the force dipole and a rotlet dipole; the hydrodynamically induced translational and rotational velocities are determined in terms of the cell body's aspect ratio, the viscosity ratio of the two fluids and the cell's distance from the boundary. This analysis predicts that pushers in the vicinity of an interface reorient and align parallel to the interfaces and swim in circular swimming trajectories.

Many recent studies of bacteria interactions with oil–aqueous interfaces were motivated by the massive Deepwater Horizon oil spill [74] from the Macondo well in the Gulf of Mexico. Surfactants were used to disperse oil droplets that were retained in sub-surface plumes; these plumes were found to be enriched with marine bacteria [75]. These bacteria are posited to have consumed long chain hydrocarbons via biodegradation [76]. Motivated by marine bacteria interaction with suspended oil droplets, Desai and Ardekani [77] perform analysis and simulation to compare the behavior of pusher-type microswimmers near a clean versus a surfactant-laden droplet. They model the swimmer as a force dipole and construct an image-singularity system to study swimmer dynamics near an incompressible Newtonian interface. They identify settings in which swimmers will scatter or interact briefly with droplets and swim away, and those in which the bacteria will become trapped adjacent to the droplets. They find that swimmers can be trapped adjacent to surfactant-laden droplets more readily than clean drops. Other studies address higher-order hydrodynamic singularities [78], and show that higher order modes, Brownian dynamics, and physicochemical interactions between the interface and swimmers further enhance bacterial accumulation near liquid interfaces (see Figure 2a). Furthermore, a source doublet and a rotlet dipole accounting for the finite size of bacteria and rotation of flagella can explain the experimentally observed bacteria body axis tilting ("nose down") near an interface [79] (see Figure 2a).

Figure 2

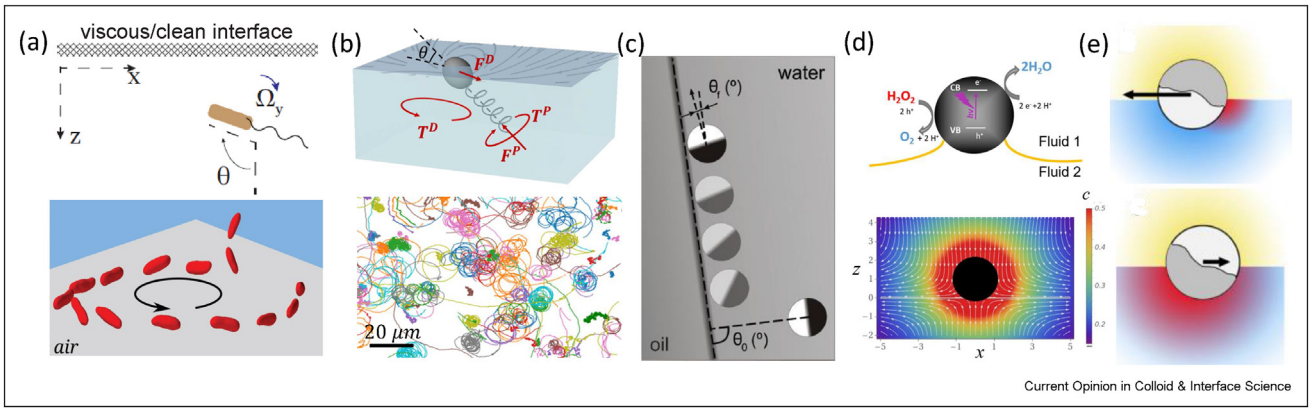

(**a**) Bacteria are hydrodynamically attracted to the fluid interfaces and reoriented near the fluid interface. The body axis of *E. coli* is observed to be tilted "nose down" near air interface (Adapted from the studies by Ahmadzadegan et al.[78], and Bianchi et al. [79]). (**b**) Force and torque balance of interfacially trapped bacteria dictates its swimming behavior. Curvilinear trajectories are observed with *P. aeruginosa* (bottom) (Adapted from the study by Deng et al. [97]) (**c**) Chemically driven Janus particle is reoriented parallel to the interface and slide along the interface (Adapted from the study by Palacios et al.[108]). (**d**) Isotropic active particle trapped at fluid interface can induce Marangoni flow that breaks its symmetry in z direction. Streamlines show the flow direction, heatmap indicates the concentration (Adapted from the study by Wittmann et al. [109]). (**e**) The propulsive speed of the interfacially trapped Janus particles depends on the steepness of the concentration gradient around the swimmers, as sketched in red. The concentration gradient is associated with the trapping configuration of the particle (Adapted from the study by Dietrich et al.[110]).

Drag asymmetry arguments like those for bacteria near solid boundaries also apply to bacteria near the fluid interfaces with viscosity contrast of two adjacent phases. This asymmetry contributes to the direction of circular paths observed near interfaces [39]. The interface between two immiscible liquids of different viscosity always features a high viscosity gradient. Microorganisms possess an ability called viscotaxis, which enables them to navigate towards regions of favorable viscosity. In a recent theoretical study, Liebchen et al. [80] proposed that viscotaxis relies on the systematic mismatch of viscous forces acting on different parts of nonuniaxial body of the swimmers, a mechanism that would be effective even for very weak viscosity gradients. In contrast, Datt and Elfring [81] argue that uniaxial swimmers, including both pushers and pullers modeled as squirmers, can display negative viscotaxis, due to the effect of viscosity gradients on the thrust generated by swimming gait. Negative viscotaxis has been observed experimentally for bi-flagellated microalgae that can reorient or scatter away from high-viscosity regions and accumulate in low-viscosity regions [82,83]. In an experimental and theoretical work [84], Lopez et al. study the behavior of helical swimmers across the viscosity gradients using synthetic helical magnetic driven swimmers. For "pusher" swimmers, the swimmer's head crosses the positive viscosity gradient followed by its tail which leads first to an increase in drag and subsequently to an increase in propulsion. Thus, the speed decreases until the tail meets the interface. The order of events is reversed for pullers entering a viscosity gradient. Pullers first experience an increase in propulsive force followed by an increase in drag on the cell body, leading to different swimming behaviors. Such viscosity gradients are sometimes coupled with a nutrient gradient which results to more complex behaviors that guided by both chemotaxis and viscotaxis [85]. The above studies address bacteria swimming *near* interfaces, which are distinct from bacteria *adsorbed on* fluid interfaces.

Bacteria adsorbed to fluid interfaces

Bacteria adhesion to oil droplets depends on the surface structure of the bacteria and the droplet's interfacial chemistry as influenced by the adsorption of surfactants or other entities at the interface, as elucidated below. For example, *E. coli* mutants with increased type I fibrae adhere more readily to both solid substrates and oil droplets over their non-mutant counterparts [86]. The adhesion of *Marinobacter hydrocarbonoclasticus* bacteria to oil droplets under flowing conditions is decreased by the addition of surfactants, with implications for bioremediation [87]. Such adhesion is enhanced by bacterial active motion [88] and is weakened by surfactant [89].

Generally, motile bacteria absorbed on interfaces of fluids that supply nutrients undergo significant changes. Initially, interfacially-trapped bacteria swim ballistically. The bacteria then change their phenotype from swimmers to sessile states, and form viscoelastic structures and pellicles reminiscent of biofilms at the oil-water interface [90–93]. For example, oil-water interfaces trigger phenotypic change of *Pseudomonas aeruginosa* from nonmucoid to mucoid cells. These changes help bacteria to shield themselves from interfacial stresses [94]. Selected mutations can favor or disfavor film formation. Niepa et al. [90] have shown that *P. aeruginosa* PA14, and

PA01 mutants lacking the alkB2 gene form an active layer under interfacial confinement, while other PA01 mutants form a passive elastic film [90]. To gain insight into the interaction and distribution of swimming bacteria with a floating viscous film on an aqueous—air interface, Desai and Ardekani [12] use a multipole representation and probabilistic simulations to show that swimmers' distribution within the films depends on their morphology and film viscosities.

Motivated by the biodegradation of oil spills, microfluidics platforms have been designed to study bacteria-oil droplet interactions under flowing conditions [95,96]. The formation of structures anchored at the interface that extend into the domain is observed. Individual, elongated, micron-scale diameter threads formed from extracellular polymeric substances (EPS) extended behind the droplet, where they captured and trapped passing bacteria. Momentum balances reveal that these structures significantly alter the pressure and increase the drag. Thus, EPS-filament decorated drops would move slowly through the water column, perhaps facilitating the relatively slow degradation process.

Bacteria swim at fluid interfaces

Motile bacteria can swim at interfaces prior to forming biofilms. Under special circumstances, for example at the interface of oil and an aqueous motility buffer with no nutrient source, bacteria can swim for prolonged times without restructuring the interface, allowing the details of their motion to be studied. Such mobile interfacial trapping has been studied by our group for motile bacteria adhered to aqueous—oil interfaces [22]. We have observed the *P. aeruginosa* PA01 in the vicinity of hexadecane—aqueous interfaces and found that most bacteria were trapped in the interfacial plane with fixed orientations of their bodies, indicating that the three-phase contact lines were pinned. The adsorbed bacteria swim along curvilinear paths with trajectory radii of curvature and speed determined by their diverse trapped configurations (see Figure 2b). Like swimmers adjacent to the interface, the rotational behavior of interfacially-trapped swimmers about an axis perpendicular to the interface is also influenced by interface impermeability and drag asymmetry due to the mismatch in the viscosity of the bulk fluids. However, pinning of the bacterial cell body and normal component of propulsive torque generated from flagellar rotation in the bulk generates another mode of circular motion independent of the hydrodynamic boundary condition. This mode leads to a faster rotation for swimmers trapped in normal configurations relative to configurations more parallel to the interface.

The forces and torques distributed around the interfacially trapped swimmers dictate their dipolar flow. In recent work, we have studied the flow field generated around interfacially-trapped swimmers [97]. One might expect the far-field flow of the trapped bacterium to be described by a fore-aft symmetric stresslet for an incompressible interface, assuming a propulsive force parallel to the interface that is balanced by drag. However, the flow field observed around an interfacially-trapped pusher bacterium has a striking lack of fore-aft symmetry. Notably, the propulsive force generated by flagellar rotation is out of the interfacial plane. This out-of-plane forcing is balanced by Marangoni stresses, giving rise to an off-interface forcing dipolar mode that contributes significantly to the observed flow field. This sum of the two dipolar modes explains the observed interfacial flow for pushers in interfaces; the modes have different weighting depending on the trapped configuration of the swimmer's bodies. Furthermore, behaviors of bacteria at fluid interfaces are also determined by cell morphology and propulsion mechanisms.

There are important open issues. While flagella dynamics of swimmers in bulk and near solids are well studied [98—103], the role of interfaces in altering flagellar dynamics is relatively unprobed. We have observed that flagellar filaments can adsorb to the interfaces or entangle with other swimmers', thus preventing their propulsive motion. Furthermore, since contact line pinning impedes swimmer reorientation and supports forces exerted on swimmers, individual flagellum and flagellar bundles can experience strong hydrodynamic forces and torques. Forces and torques generated by the force dipole or rotlet near the interfaces [104], or from hydrodynamic interactions with other swimmers can lead to rearrangement of the flagella. In addition, the interface could restructure the flagellum in other ways. Flagella undergo known instabilities in bulk fluids. For monotricous bacteria, the propulsive force from the fluid on the flagellum transmits to the elastic hook and induces buckling when above a critical threshold for bacteria to reorient themselves [105,100]. For peritrichous bacteria that perform run-and-tumble motion, flagellar bundling and unbundling are modeled in terms of hydrodynamic and electrostatic interactions between flagellar filaments [106]. Such flagellar structural dynamics are likely altered near fluid interfaces.

The motion of other microorganisms near interfaces is yet to be understood. For example, magnetotactic bacteria (MTB) contain an array of magnetic nanoparticles or magnetosomes that allow them to orient in magnetic fields [107]. The interplay of magnetic torque and hydrodynamic torque due to self-propulsion near boundaries may lead to different swimming dynamics. The magnetic field can also guide their motions and suppress the fluctuation in the direction of their active motion. These features suggest that MTB near fluid interfaces would be an excellent model system to study to direct swimmer interactions and collective motion. The bacteria species *Thiovulum majus*

would also be an excellent model system to study self-organization and interfacial mixing of active colloids. These bacteria have large spherical bodies covered with ~100 relatively short flagella that enable them to swim as fast as 600 μm/s.

Janus and catalytic swimmers

Phoretic swimmers are an important class of synthetic swimmers that generate a scalar gradient through surface reaction. The inhomogeneous scalar field around the particle, for example the chemical concentration, temperature, or electrostatic potential can generate a nonzero slip velocity at the particle surface, thus inducing force- and torque-free propulsion in the bulk. Such self-propulsion can be achieved by designing Janus particles that break the fore-aft symmetry, such as metal-coated hemispheres [111], or bimetallic rods [112], to generate non-uniform distribution of reaction products, temperature, etc. along the surface. The far-field flow of these self-propelled particles can be modeled as a force dipole [9,113]. Such swimmers are predicted to have hydrodynamic entrapment and curvilinear trajectories near interfaces like pusher bacteria [114]. However, flow can alter the ion or reactant transport [113], affecting their motion. Thus, the interactions between the swimmer–swimmer and swimmer-interface are governed by the interplay of hydrodynamic and phoretic effects.

When particles straddle fluid interfaces, their behaviors are strongly affected by the particles' trapped configurations which determine the phoretic solvent flow bounded by the fluid interfaces and the redistribution of chemically active molecules across the two phases. Synthetic catalytic swimmers follow complex paths at interfaces, with their propulsive mechanisms influenced by their adsorbed state. For example, platinum–silica Janus particles powered by decomposition of hydrogen peroxide (H_2O_2) as chemical fuel can become trapped at air–water interfaces with random orientations. When no chemical fuel is present in the system, they tend to adsorb to the interface with their platinum-caps facing oil [115]. Once adsorbed, contact line pinning permits translation along the interface and rotations around axes normal to the interfaces. Active particles at interfaces are found to swim with either rectilinear trajectories or circular trajectories [116]. Their rotational behavior can be generated by their broken symmetry along the propulsive axis due to the anisotropic particle shape [117,116], and can also be generated from far-field hydrodynamics due to the drag asymmetry near fluids with different viscosity [118]. Numerical analysis of the self-diffusiophoretic behavior of colloids trapped at interfaces shows that nonuniform velocity across the interface can generate net torque on the colloid even in the absence of viscosity contrast between two phases [119].

As phoretic colloids swim on interfaces, chemical fuel is redistributed around the swimmer, limited by mass transport across the interfaces. The chemical gradient around the swimmer is sensitive to the position of the catalytic site which further constrains the self-propelled motion. For example, Dietrich et al. shows that a smaller platinum site in the water phase generates steeper gradients of reactants and products of H_2O_2 [110], which leads to an increased swimming speed (see Figure 2e). The directional active motion of Janus particles is also associated with the Brownian rotational diffusion which minimizes the active transport of particles. The irreversible adsorption of Janus particles at fluid interfaces limits the rotational degrees of freedom, thus slowing the rotational diffusion and enhancing the persistency of their directional behaviors [120,118,110]. Stocco et al. propose a possible mechanism that relates the reduced rotational diffusion observed in experiment to contact line fluctuations and wetting-dewetting dynamics that cause larger rotational contact line friction [31].

Although artificial swimmers and natural swimmers are predicted to behave similarly in terms of their far-field hydrodynamics as self-propelled objects, the dependence of their propulsion mechanism on transport near the interface generates different swimming behaviors near solid walls and fluid interfaces. Near solid surfaces, wall-induced distortion of the chemical field around the particle modifies the hydrodynamic flow, thus inducing stable behaviors of Janus particles including "sliding" [121] and "hovering" above a wall [122]. The chemical gradient near the solid surface can also generate osmotic flows that reorient and dock swimmers at the wall [123]. Near fluid interfaces, differing solubilities of chemicals in the adjacent fluid phases also induces active reorientation and persistent sliding [115,124,108] next to the interfaces (see Figure 2c) and the pinning line of oil droplet sitting on the surfaces [124]. Furthermore, the molecules that drive phoresis can also adsorb to the fluid interfaces, where they can change the local surface tension and induce Marangoni stresses along the interfaces.

Homogeneous catalytic particles in bulk with uniform concentration of reactants act as spherically symmetric sources or sinks of chemical reactants. Absent broken symmetries, these particles are predicted to show no net displacement. However, near fluid interfaces, theory predicts that broken symmetries can induce self-phoresis of particles by distorting the local distribution of chemical species and changing the local velocity profile (see Figure 2d) [125,126,109]. Homogeneous particles can be attracted to or repelled from interfaces. The attraction or repulsion depends on ratio of the diffusivities, solubilities of the catalysis products in the two coexisting phases, and the effect of the chemical species on modifying the surface tension. Daddi-

Moussa-Ider et al. [127] also proposed the self-diffusiophoretic motion of isotropic catalytic particle near a finite-sized disk trapped at fluid interfaces. Thus, the swimming behavior can be tuned by changing the geometrical properties of the system, e.g., the disk size. Similarly, behaviors of the non-homogeneous particles oriented normal to the interfaces are determined by their intrinsic swimming velocity and the interface induced velocity. The competition between these two effects, which depends on the surface coverage of catalytic sites [125], can lead to a steady-state hovering over the interfaces.

There is a tremendous body of work on Janus particles that can be exploited and unified with the design Janus phoretic swimmers to dictate structure formation and interface response. Janus particles have been engineered to adsorb spontaneously to reduce the surface tension and stabilize the interfaces in order to generate particle-stabilized emulsions and foams, [128−131]. The implications of their translational and rotational dynamics have been studied in the context of assembly at fluid interfaces [132,133] and harnessed to design interfaces with different stability and rheology. Janus particle adsorption and assembly at fluid interfaces are guided by hydrophobic interactions, electrostatic interactions, and capillary interactions. These interactions can be tuned via the geometry and surface properties of the particles [128]. Hydrodynamic and phoretic interactions induced by active Janus particles can generate strong and long ranged interactions that can be tuned by chemical composition and physical properties of the two fluid phases. Studies that unite the fields of Janus particle design and phoretically active Janus beads will have additional interactions to tune particle structure formation and effective properties at fluid interfaces.

Marangoni surfers

Marangoni surfers are bound to the fluid interfaces, and move under broken symmetries generated in the surface tension around them. The Marangoni propulsion mechanism has been observed in water-floating natural creatures [134] and is widely used in artificial systems, as it allows a wide range of propulsion speeds [135] and precise manipulation of particle dynamics [136]. The nonuniform surface tension around the Marangoni surfer may arise from a surface gradient in temperature [137−139,135,140], chemical potential [141−144,142,143,145,146] or electrostatic potential [147,148]. In these systems, inertia and bulk advection [149,150] are typically important, generating elongated concentration boundary layers [151,152] or thermal boundary layers [135] that alter surfer dynamics (Figure 3a). In a study of thermocapillary driven motion, Dietrich et al. observed propulsion velocities up to 10^4 body lengths per second (on the order of cm/s) due to thermal gradients generated by high power illuminated from light [135]. At these velocities, *Pe* are elevated, and Marangoni surfer motion is dominated by advection, with weaker dependence on their intrinsic asymmetry [146,153,154]. These authors also find that the effect of surfactants is inevitable. Marangoni stresses due to surfactant redistribution resist the thermal Marangoni stresses, thus slowing the Marangoni swimmers [135].

The non-uniform tension creates a net surface force on the colloid, and also generates a long-range Marangoni flow [155,156,156]. The hydrodynamic drag on the surfer due to this flow can contribute to, or impede surfer propulsion [156,155,157,156], and can even propel them in the direction of lower surface tension direction [150,158]. For example, Jafari Kang et al. recently related the bulk flow around a chemically driven Marangoni surfer to its forward, reverse, and arrested motion [150]. Their experimental observations are supported by numerical simulations, shown in Figure 3b, which reveal the negative pressure gradients in the subphase generated by divergent flow behind the swimmer to drive the reverse motion of Marangoni swimmers.

Driven colloids and microrobots

Colloidal motion can also be directed by external fields, including magnetic, acoustic and electric fields. Furthermore, interactions between the external fields and colloids or their surrounding environments can drive unique dynamics behaviors of the system. Driven colloids at interfaces are influenced by the presence of long-ranged hydrodynamic and other physicochemical interactions that make them ideal model elements for fundamental study of their motion, self-assembly, and non-equilibrium dynamics. These insights are exploited to generate active functional structures and micro-robots.

External magnetic forces have been used to direct ferromagnetic, interfacially-trapped micro-robots on the scale of hundreds of microns to manipulate colloidal cargo at interfaces via capillary and hydrodynamic interactions [162,23]. However, prohibitively strong magnetic field gradients can be required to translate smaller, microscale colloidal particles. Thus, rather than exploiting magnetic forces, magnetic torques are commonly exploited. Under a static field, dipole−dipole repulsion among aligned magnetic moments of interfacially-trapped colloids causes a two-dimensional lattice structure to form [163]. Fields rotating in the plane of the interface trigger complex interparticle interactions. For example, early works by Grzybowski et al. [164,165] demonstrated that millimeter sized rotating disks at interfaces assembled into dynamics structures guided by an interplay of hydrodynamic repulsion and magnetic attraction. More recently, Wang et al. designed magnetic micro-rafts of 50 μm radius with engineered edge−height profiles to generate repulsive capillary interactions under high frequency rotating magnetic fields

Figure 3

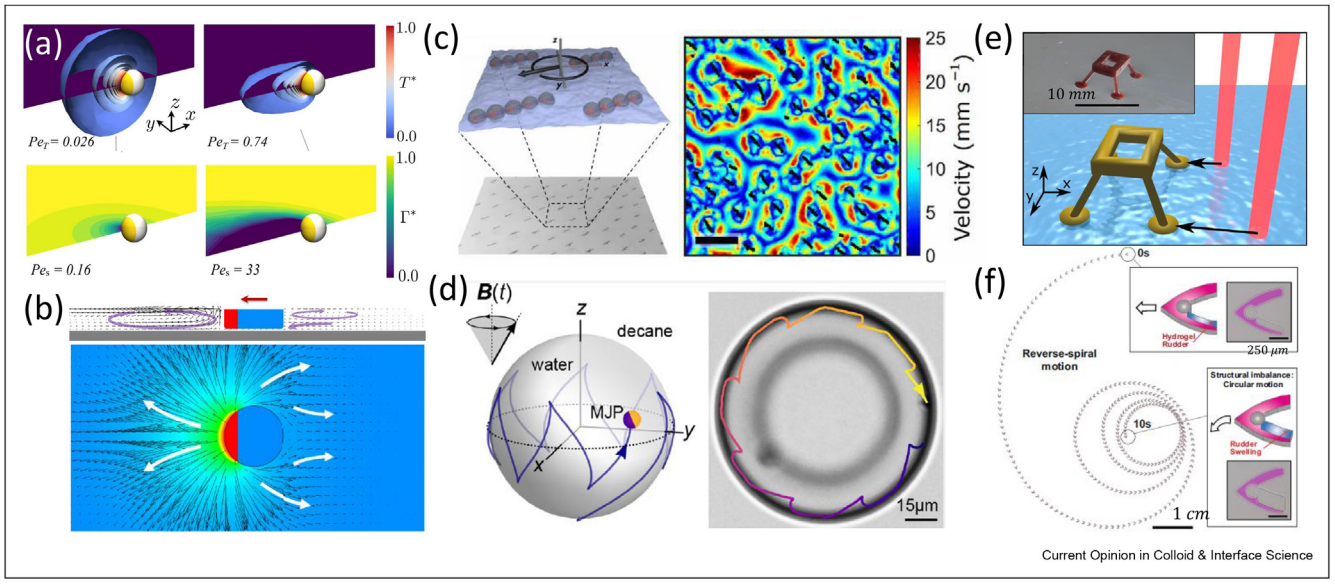

(**a**) Marangoni surfers swim with finite Peclet number demonstrate a stretched region of temperature gradient or surface concentration gradient [135]. (**b**) Side view and top view of a Marangoni propelled disk under confinement. The counterclockwise rotating vortex in the wake of the surfer generates negative pressure that drives reverse propulsion [150]. (**c**) Magnetic particles assemble into active spinners under a rotating magnetic field. The self-assembled spinners locally inject vorticity into the liquid interface and generate strong hydrodynamic flows. (Adapted from the study by Han et al. [159]). (**d**) Time-varying magnetic field leads to different motion of magnetic particle at the interface of oil droplet [160]. (**e**) A floating microrobot controlled by two separate laser sources that generate thermocapillary flow [161]. (**f**) A microrobot achieves time-dependent motion by controlling the release of chemical fuel using photopatterning method [136].

[116]. The balance of magnetic attraction and capillary repulsion allowed dynamic assembly of multiple micro-rafts which could be further programmed by tuning the objects' initial positions and the frequency of the rotating fields. Unlike the micro-rafts, spherical ferromagnetic colloids trapped at interfaces assemble into chain-spinners under a rotating field. The chain lengths depend on the field frequency [159]. In a certain frequency range, the chains spin synchronously within the external magnetic field and generate strong hydrodynamic flows with potential as mixers at the interface (shown in Figure 3c). Multiple spinners formed dynamic lattices with features that include self-healing and enhanced transport of embedded cargo particles. More recently, He et al. exploited chains of ferromagnetic disks assembled under a rotating field as active elements. Under a precessing field, these chains acted as micropaddles, and moved along the interface. The micropaddles were harnessed for micro-manipulation of adsorbed colloidal cargo [166].

In magnetic fields oscillating perpendicular to the interface, forces on particles with pronounced magnetic moments can drive interfacial deformation. These deformations drive neighboring particles to form magnetic "snakes" [167,168], or dynamic asters [169] via capillary interactions. Such structures can generate strong hydrodynamic flow that further promotes assembly or induces translation [8]. More recently, many–body interactions between adsorbed superparamagnetic colloids were exploited and controlled by changing the tilt angle of external magnetic fields to generate aggregates, carpets, and other assemblies [170,7]. Curved fluid interfaces can also guide reorientation of anisotropic particles to minimize the interfacial energy, and rotation of asymmetric particles can generate translation via broken symmetries. The motion of adsorbed magnetic Janus particles on oil droplets was achieved by controlling the frequency and titled angle of the magnetic field and particle position (Figure 3d) [160,171].

Microrobots moving on interfaces have been developed that exploit such interactions to perform tasks including capture, transport, release and assembly of colloidal building blocks. Hybrid actuation strategies for robust and controllable actuation of micro-objects at interfaces have been developed. Such studies exploit precise control of microrobotic motion and "physical intelligence" [19] in the form of active-passive colloid interactions to guide assembly and to manipulate cargo. For example, magnetic microrobot shape can be designed to generate interfacial curvature and long-ranged capillary attraction to specific sites at capture, dock, and transport colloidal cargo. Cargo can be released by micro-robot rotation and delivered to building sites or assemblies guided by capillarity. Cargo capture is influenced by capillary interactions and hydrodynamic advection [23]. Several challenges arise for

designing floating microrobots. For example, capillary interactions can impede the cargo release and patterned assembly. Complex stress conditions and interplay between different interactions make precise microrobot control difficult. To overcome these hurdles, floating microrobot pairs have been developed with preferred magnetization direction to allow precise control of their position and orientation using a single permanent magnet [172]. The microrobots' shapes were designed to prevent strong near-field interactions and to allow grasping, alignment, positioning and release of floating functional elements by tuning the microrobot separation distance. Micro-disk collectives driven by time-varying magnetic particles can rotate, oscillate, remain static, form structures, or navigate through confined spaces [6].

More complicated hybrid systems have been designed in which capillary interactions are integrated with other effects, including Marangoni effects. For example, a floating microrobot with multiple legs was actuated by separate laser spots to control force and torque exerted on the microrobot [161]. The programmable laser system induced temperature gradients and localized Marangoni flow to micromanipulate locomotion and to direct assembly (Figure 3e). In another study, microrobots were designed to precisely release surface active molecules, thus achieving programmable motion [136] (Figure 3f).

Interactions, collective behaviors and applications

Colloidal assembly

Several distinct physico–chemical interactions play important roles on the colloidal length scale, many of which are strongly changed by particle trapping at interfaces. For example, the dissociation of surface groups on particles is asymmetric across the interface. This gives rise to electric dipoles on adsorbed particles oriented perpendicular to the interface, and leads to repulsive electrostatic interactions between them. The resulting long-ranged dipole–dipole interactions drive particles to form a crystalline lattice at the interface that is affected by surface properties of the particles and additives in bulk phases [176,21]. Hydrodynamic interactions also influence assembly [177]. In the near field, surfactants or macromolecules can be adsorbed uniformly to form soft corona on hard-core particles [178] or to form patchy islands [179] for directed interactions. Other interactions, like capillary interactions or Marangoni propulsion, rely on surface tension or its gradients that occur only in fluid interfaces. Often, several of such interactions are present on adsorbed colloids simultaneously and offer important degrees of freedom for engineering interfacial systems.

Active particles can guide the organization of passive colloids through active-passive interactions [180], e.g., capillary interaction, hydrophobic interaction, and magnetic interactions, and direct the assembly of passive colloids [23]. Active particles can also interact with organized structures formed by passive colloids in the interface and affect their microstructure. For example, Dietrich et al. [173] studied the motion of self-propelled Janus particle in a two-dimensional colloidal crystal stabilized by dipole–dipole electrostatic interactions between passive colloids. The phoretic Janus particle can couple with the lattice through electrostatic dipolar interactions, whose magnitude depends on the charge distribution around Janus particle and the orientation of its catalytic site. For weak coupling, Janus particles navigate through the crystal in a run-and-tumble like fashion, due to the reorientation effect from collision to the obstacles. Large coupling between an active particle and a colloidal crystal results in an intermittent motion of the swimmer and structural rearrangement of the monolayer (Figure 4a). In another example, Martinez-Pedrero et al. [181] studied the collective behaviors of two types of magnetic particles that adsorb at different vertical positions of the interfaces. By applying an elliptically polarized precessing magnetic field, the particle lattice formed by larger magnetic particles can translate on the interface. The strong coupling between the active and passive magnetic particles leads to collective transportation of small magnetic particles in the lattice. In both studies, the hydrodynamics effect of active particles is neglected, which can play important role in colloidal structure formation, and long-ranged collective behaviors [182,183].

Collective behaviors

Recent studies of Marangoni surfers address collective dynamics at interfaces. Marangoni surfers can generate bulk vortical flows that attract the neighboring particles [184], while local reduction of surface tension can generate repulsive interactions between particles, thus driving colloidal crystal formation [185,174] (Figure 4b). Hydrodynamic interactions from Marangoni flows compete with the rotational diffusion of particles [186] and diverse particle interactions, e.g., capillary interactions, and electrostatic interactions can tune the structures formed in colloidal monolayers and their stability [187,188,174,189]. Rich collective behaviors and pair interactions are observed experimentally, such as synchronization [144,190], assembly [191,185], and cluster formation [109,192–194], which depends on the direction of the activity-induced Marangoni flow. Collective behaviors also emerge among homogeneous chemically-or thermally-driven particles. Perturbation by neighboring particles of concentration or thermal field can break the system's symmetry and induce collective motion [184,195,109,188,174]. Dynamics of sparse Marangoni surfers' assemblies differs from that of living matter. Velocities around Marangoni surfers display turbulent-like behavior (Figure 4c) [175] that is different from the active turbulence generated by self-

Figure 4

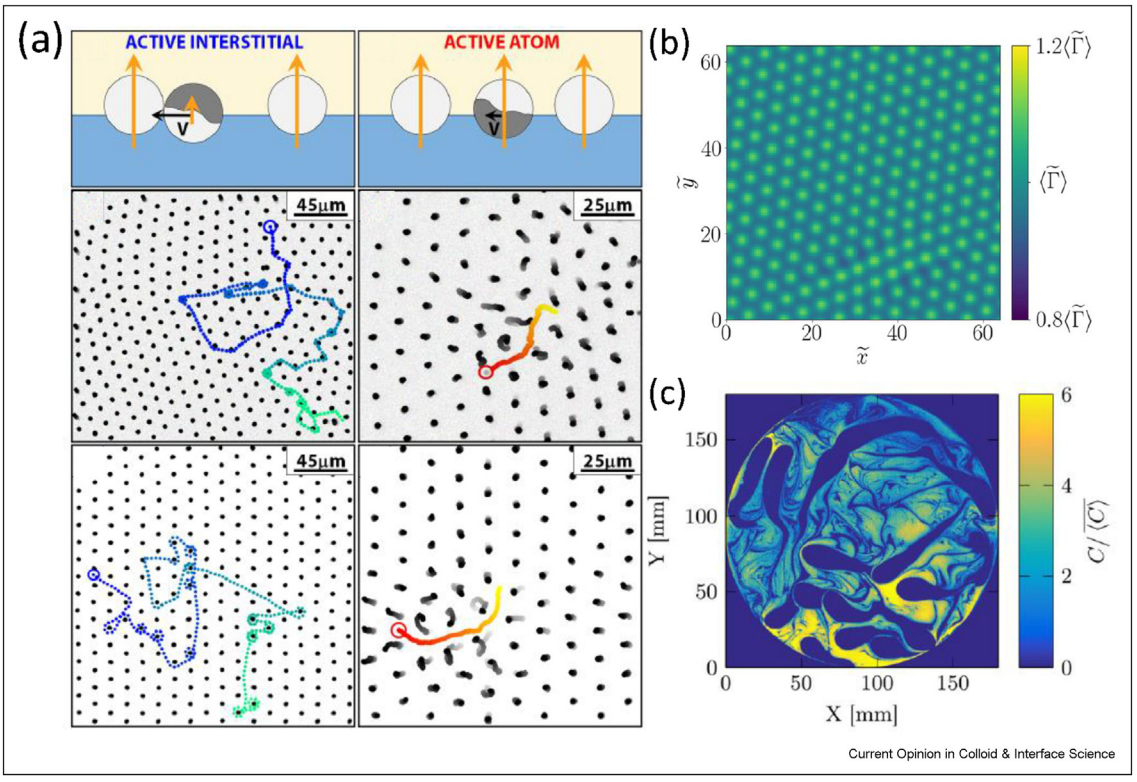

(**a**) Active Janus particles swimming in hexagonally packed colloidal crystals present two types of swimming behaviors depending on the strength of coupling between active particle and colloidal monolayer [173]. (**b**) Many body interactions between Marangoni swimmers can lead to colloidal crystals [174]. (**c**) The camphor swimmers create "turbulentlike"concentration spectra, with a large-scale region, an inertial regime, and a Batchelor region [175].

propelled swimmers. Rather, the behavior bears the signatures of an inertial turbulence regime [196].

Self-propelled objects, including bacteria and Janus particles show spatial−temporal chaotic organization, whose motion is correlated at large scales [13]. Their collective behaviors are not yet widely addressed at fluid interfaces. However, there are a number of studies in bulk and at solid surfaces that suggest interesting directions for future study. In dense systems, self-propelled particles self-organize into mesoscale turbulent structure via active realignment of neighboring particles or other short−range interactions including lubrication forces, steric repulsions and physical entanglement [13]. In a relatively dilute limit, hydrodynamic pair interactions for natural swimmers or phoretic interactions for Janus swimmers [197] can generate attraction or repulsion that drives cluster formation or scattering. Near solid walls, collective motion is constrained by the wall confinement [198−200]. For example, hydrodynamic interactions have been studied between magnetotactic bacteria in dilute suspension oriented perpendicular to solid boundaries by an external field [201]. The solid wall imposes a net force that balances the flagellar thrust of the trapped bacterium. The dominant flow is described by a Stokeslet near the wall which induces attractive interactions among neighboring swimmers and leads to cluster formation. In dense suspension, Thery et al. [202] observed that such clusters grow and form plumes that advect bacteria through a backward flow. The plumes also interact with each other and merge into larger plumes. Hydrodynamic clustering has also been observed for *T. majus*. However, these bacteria remain in surface-bound states and form two-dimensional rotating crystals instead of three-dimensional plumes [45] due to their special cell morphology. Fluid interfaces offer unique mechanisms to influence collective motion. For example, interfaces can confine the active suspensions and guide their behaviors through local curvature. Non-equilibrium trapping states and interfacial stresses can lead to complex interactions between swimmers. For example, adsorbed bacteria aligned perpendicular to the interface can rotate rapidly in a relatively fixed location with its propulsive force balanced by the capillary force [22]. In the "clean" interface limit, the perpendicular swimmer can generate "sink-like" dipolar flow on the interfaces that can attract other swimmers [40]. However, the interfacial incompressibility resists any inward flow, which may lead to completely different dynamics

of collective behaviors than near solid walls. The collective effects for swimmers at interfaces remain unprobed.

Enhanced transport in application

There are exciting opportunities to design interfaces for enhanced transport in multiphase systems. For example, emulsion droplets in which drop phase and continuous phase solvents have differing polarities have been exploited for process intensification schemes in which a reactant in the droplet phase forms a product that is soluble in the external phase. In these settings, reaction and separation occur simultaneously at the droplet interface [203]. Active colloids at interfaces could be designed as active surface agents with the potential to promote local mixing, enhance surface reaction rates and enhance transport between the phases. External fields applied to the interfaces, or active motion of individual swimmers can drive the system far from equilibrium which induce micromixing or drive target delivery [20,128,204,203].

Hydrodynamics of isolated swimmers and interactions between swimmers and passive tracers reveal enhanced transport in liquid suspension; passive tracers display enhanced diffusivity and non-Gaussian statistics that differ from thermally driven Brownian motion. The seminal work conducted by Wu and Libchaber [205] identified the initial super-diffusive regime in the mean squared displacements of tracer particles in bacterial suspension in thin liquid films. The duration of the superdiffusive regime is far longer than that generated by thermal fluctuation, and depends on swimmer concentration. Tracers are entrained by swimmers' through far-field flows [206,207] and advected along loopy trajectories, and jump in low-frequency collision from the swimmer [208]. The non-Gaussian behaviors and diffusion of passive tracers at fluid interface show unique features, including swimmer-driven oscillatory tracer trajectories that generate prolonged subdiffusive plateau in the tracers' MSD [97]. Tracer behaviors are not only modified by the induced flow around the swimmers bounded by fluid interfaces. Tracer motion is also influenced by unique features of swimmer motion at interfaces. For example, contact line pinning of swimmers can stabilize the active motion, reduce the rotational diffusivity, promote swimming in circular pathways and allow the swimmers to interact persistently with passive tracers. Active swimmers can undergo "self-caging" in their net displacements due to their curvilinear trajectories; thus, they displace the passive tracer in an oscillatory manner. The significance of convective flow generated by swimmers compared to the diffusion of passive tracers or small molecules can be evaluated using Peclet number (Pe) defined in terms of the flow generated by isolated swimmers. Microscale self-propelled swimmers with propulsive speed $\sim$ 10 μm/s and fluid velocity that decays with $1/r^2$ can hydrodynamically advect passive colloidal particles, enhancing their mixing. For small molecules, which have faster diffusion, $Pe \ll 1$, and the enhanced transport is negligible. However, in dense active suspensions, coherent structures emerge which generate strong recirculatiing flows with slower decay rates that enable large-scale transport of molecules [11,16]. In this limit, a mere superposition of hydrodynamic contributions from individual swimmers is not suitable, and complex multibody effects must be considered. A challenge in this field will be predicting transport driven by active clusters in order to design active structures that promote transport.

Conclusions and outlook

The highly anisotropic environment of fluid interfaces, and the tendency of active colloids to become trapped near or on interfaces generate dynamics that differ fundamentally from their bulk counterparts. As we deepen our understanding of these dynamics, we also develop criteria to design active surface agents to generate new modes of interfacial response. In all aspects of active colloids at interfaces, there are important open issues and opportunities for application that remain to be developed. We underscore some of these concepts here.

As we deepen our understanding of active and driven colloid motion in relation to the stress state and rheology of the interface, new tools with greater precision in characterizing interfaces will emerge at the colloidal and molecular scale. The similarities between active colloids at interfaces and active proteins in lipid bilayer membranes might inspire new approaches to active colloid assembly at interfaces.

While we have improved our understanding of swimmers at interfaces, and have identified the importance of contact line pinning, off-interface forcing, and interfacial stresses, there are predicted hydrodynamic modes that have not yet been observed. One mode, in particular, is the asymmetric dipolar mode that induces no interfacial flow but generates a "pumping flow" in the adjacent phases [40]. This mode could have implications in nutrient capture for interfacially trapped bacteria, and could be harnessed for micromixing in biomimetic systems.

While the swimming trajectories and hydrodynamics of individual bacteria have been addressed in theory and experiment, the effect of fluid interfaces on the propulsive performance of flagellar filaments is lacking. Experiments designed to address these effects could probe the manner in which interfacial trapping alters flagella stability or bundling behaviors.

Solid boundaries are known to alter the collective dynamics of active colloids. However, the behavior of

active colloidal suspensions at fluid interfaces, in particular suspensions of self-propelled colloids near or on interfaces is significantly less developed.

In biomimetic systems, there are important open opportunities to the rapidly-evolving insights into swimmer dynamics at interfaces. The ability to design interfaces to incorporate self-propelled colloids as truly active surface elements, self-propelled objects that accumulate, adsorb, and move, could revolutionize interfacial engineering by providing news means of enhancing interphase transport and functionality with impact in fields including food, pharmaceuticals, and personal care industries. Fundamental studies to guide this design can exploit the improved understanding of swimming at interfaces that is emerging in the literature. As artificial active colloids develop, the community can develop criteria for selecting the strengths of various dipolar modes, interface mechanics, and propulsion modes to promote structure formation and cargo attachment in the interface or dissemination and release of cargo.

The concept of swimmer-propelled droplets also deserves greater exploration both in theory and in experiment. This opens the exciting prospect of active emulsions and should generate increased study in the field. The intersection of these studies with reaction/separation schemes based on droplets containing reactants that generate products soluble in the external phase could lead to chemical processes with improved productivity.

We have focused on bacteria at interfaces as model swimmers and noted many ways in which interfaces constrain their motion. More generally, in nature, the ability of an organism to maneuver can determine its ability to gather nutrients, escape predators, and ultimately survive. Furthermore, the ability of an organism to sense neighbors, form colonies and enter sessile states can confer other advantages. Bacteria at interfaces can move, interact, assemble, change phenotype and form colonies and films, with early-stage behaviors that differ from solid surfaces significantly. The importance of bacterial trapping and association with interfaces in biology is far less developed than at solid boundaries and should be considered in the broader context of bacterial mechanosensing [209] and considered in light of the chemical complexity of fluid interfaces.

In conclusion, active colloids at interfaces present important opportunities for interfacial engineering and for fundamental study with exciting real-world applications.

Declaration of competing interest

The authors declare that they have no known competing financial interests or personal relationships that could have appeared to influence the work reported in this paper.

Acknowledgment

This work is supported by National Science Foundation (NSF grant no. DMR-1607878 and CBET-1943394).

References

Papers of particular interest, published within the period of review, have been highlighted as:

* of special interest
** of outstanding interest

1. Fuller GG, Vermant J: **Complex fluid-fluid interfaces: rheology and structure**. *Annu Rev Chem Biomol Eng* 2012, **3**:519–543, https://doi.org/10.1146/annurev-chembioeng-061010-114202. https://www.annualreviews.org/doi/10.1146/annurev-chembioeng-061010-114202.

2. Lapointe CP, Reich DH, Leheny RL: **Manipulation and organization of ferromagnetic nanowires by patterned nematic liquid crystals**. *Langmuir* 2008, **24**:11175–11181, https://doi.org/10.1021/la801818x. https://pubs.acs.org/doi/10.1021/la801818x.

3. Dhar P, Cao Y, Fischer TM, Zasadzinski JA: **Active interfacial shear microrheology of aging protein films**. *Phys Rev Lett* 2010, **104**, 016001, https://doi.org/10.1103/PhysRevLett.104.016001. https://link.aps.org/doi/10.1103/PhysRevLett.104.016001.

4. Choi S, Steltenkamp S, Zasadzinski J, Squires T: **Active microrheology and simultaneous visualization of sheared phospholipid monolayers**. *Nat Commun* 2011, **2**:312, https://doi.org/10.1038/ncomms1321. http://www.nature.com/articles/ncomms1321.

5. ** Spatafora-Salazar A, Lobmeyer DM, Cunha LHP, Joshi K, Biswal SL: **Hierarchical assemblies of superparamagnetic colloids in time-varying magnetic fields**. *Soft Matter* 2021, **17**: 1120–1155, https://doi.org/10.1039/D0SM01878C. http://xlink.rsc.org/?DOI=D0SM01878C.
This is a recent review paper on using time-varying magnetic field to tune the interactions between superparamagnetic particles and guide their hierarchical assemblies into different structures

6. * Gardi G, Ceron S, Wang W, Petersen K, Sitti M: **Microrobot collectives with reconfigurable morphologies, behaviors, and functions**. *Nat Commun* 2022, **13**:2239, https://doi.org/10.1038/s41467-022-29882-5. https://www.nature.com/articles/s41467-022-29882-5.
Using time-varying magnetic field, the authors can drive micro-disk collectives to different behaviors, form structures, or navigate through confined space

7. ** Martínez-Pedrero F: **Static and dynamic behavior of magnetic particles at fluid interfaces**. *Adv Colloid Interface Sci* 2020, **284**, 102233, https://doi.org/10.1016/j.cis.2020.102233. https://linkinghub.elsevier.com/retrieve/pii/S0001868620304048.
This review paper focus on the response of magnetic particles at fluid interfaces under controlled external fields, and their implications in interfacial transport, active rheology and structure formation

8. Snezhko A: **Complex collective dynamics of active torque-driven colloids at interfaces**. *Curr Opin Colloid Interface Sci* 2016, **21**:65–75, https://doi.org/10.1016/j.cocis.2015.11.010. https://linkinghub.elsevier.com/retrieve/pii/S1359029415000990.

9. Lauga E, Powers TR: **The hydrodynamics of swimming microorganisms**. *Rep Prog Phys* 2009, **72**, 096601, https://doi.org/10.1088/0034-4885/72/9/096601. https://iopscience.iop.org/article/10.1088/0034-4885/72/9/096601.

10. Utada AS, Bennett RR, Fong JCN, Gibiansky ML, Yildiz FH, Golestanian R, Wong GCL: **Vibrio cholerae use pili and flagella synergistically to effect motility switching and conditional surface attachment**. *Nat Commun* 2014, **5**:4913, https://doi.org/10.1038/ncomms5913. http://www.nature.com/articles/ncomms5913.

11. Mathijssen AJ, Guzmán-Lastra F, Kaiser A, Löwen H: **Nutrient transport driven by microbial active carpets**. *Phys Rev Lett*

2018, **121**, 248101, https://doi.org/10.1103/PhysRevLett.121.248101. https://link.aps.org/doi/10.1103/PhysRevLett.121.248101.

12. Desai N, Ardekani AM: **Biofilms at interfaces: microbial distribution in floating films**. *Soft Matter* 2020, **16**:1731–1750, https://doi.org/10.1039/C9SM02038A.
** The authors studied bacteria distribution along the viscous film at fluid interfaces using multipole representations and probabilistic simulations. Bacterial distribution depends on its cell morphology and whether it is pusher or puller

13. Alert R, Casademunt J, Joanny J-F: *Active Turbul, Annu Rev Condens Matter Phys* 2022, **13**:143–170, https://doi.org/10.1146/annurev-conmatphys-082321-035957. https://www.annualreviews.org/doi/10.1146/annurev-conmatphys-082321-035957.
** This recent review focuses on the self-organized nature observed in active matter, including bacterial suspension, swarming sperm, microtubules and molecular motors, tissue cells and artificial swimmers. Differences between active turbulence and inertial turbulence are emphasized.

14. Krsmanovic M, Biswas D, Ali H, Kumar A, Ghosh R, Dickerson AK: **Hydrodynamics and surface properties influence biofilm proliferation**. *Adv Colloid Interface Sci* 2021, **288**, 102336, https://doi.org/10.1016/j.cis.2020.102336. https://linkinghub.elsevier.com/retrieve/pii/S0001868620306059.

15. Kokot G, Das S, Winkler RG, Gompper G, Aranson IS, Snezhko A: **Active turbulence in a gas of self-assembled spinners**. *Proc Natl Acad Sci USA* 2017, **114**:12870–12875, https://doi.org/10.1073/pnas.1710188114. https://pnas.org/doi/full/10.1073/pnas.1710188114.

16. Sokolov A, Apodaca MM, Grzybowski BA, Aranson IS: **Swimming bacteria power microscopic gears**. *Proc Natl Acad Sci USA* 2010, **107**:969–974, https://doi.org/10.1073/pnas.0913015107. https://pnas.org/doi/full/10.1073/pnas.0913015107.

17. Fu S, Wei F, Yin C, Yao L, Wang Y: **Biomimetic soft microswimmers: from actuation mechanisms to applications**. *Biomed Microdevices* 2021, **23**:6, https://doi.org/10.1007/s10544-021-00546-3. http://link.springer.com/10.1007/s10544-021-00546-3.
** This recent review focuses on the various actuation mechanisms of natural swimmers, including fish-like, snake-like, jellyfish-like and microbial-inspired ones. They summarize the changes and potential applications of these microrobots in real environments

18. Johnson AP, Sabu C, Nivitha K, Sankar R, Ameena Shirin V, Henna T, Raphey V, Gangadharappa H, Kotta S, Pramod K: **Bioinspired and biomimetic micro- and nanostructures in biomedicine**. *J Contr Release* 2022, **343**:724–754, https://doi.org/10.1016/j.jconrel.2022.02.013. https://linkinghub.elsevier.com/retrieve/pii/S0168365922000888.

19. Sitti M: **Physical intelligence as a new paradigm**. *Extreme Mech Lett* 2021, **46**, 101340, https://doi.org/10.1016/j.eml.2021.101340. https://linkinghub.elsevier.com/retrieve/pii/S2352431621001012.
** A short review paper introducing the concept of "Physical Intelligence" (PI), its application in many research fields, such as active matter, biology and self-assemblies, etc

20. Fei W, Gu Y, Bishop KJ: **Active colloidal particles at fluid-fluid interfaces**. *Curr Opin Colloid Interface Sci* 2017, **32**:57–68, https://doi.org/10.1016/j.cocis.2017.10.001. https://linkinghub.elsevier.com/retrieve/pii/S135902941730016X.

21. Guzmán E, Martínez-Pedrero F, Calero C, Maestro A, Ortega F, Rubio RG: **A broad perspective to particle-laden fluid interfaces systems: from chemically homogeneous particles to active colloids**. *Adv Colloid Interface Sci* 2022, **302**, 102620, https://doi.org/10.1016/j.cis.2022.102620. https://linkinghub.elsevier.com/retrieve/pii/S0001868622000227.
** A broad review on particle dynamics at fluid interfaces, including particle adsorption, inter-particle interactions and mechanical response of the particle–laden interfaces. Based on the fundamental understanding, they also introduce potential applications of particles confined at interfaces

22. Deng J, Molaei M, Chisholm NG, Stebe KJ: **Motile bacteria at oil–water interfaces: *Pseudomonas aeruginosa***. *Langmuir* 2020, **36**:6888–6902, https://doi.org/10.1021/acs.langmuir.9b03578. https://pubs.acs.org/doi/10.1021/acs.langmuir.9b03578.
* Individual swimming behaviors of motile bacteria P.aeruginosa are studied and characterized into four types, including: curly motion, pirouettes, diffusive and interfacial visitors

23. Yao T, Chisholm NG, Steager EB, Stebe KJ: **Directed assembly and micro-manipulation of passive particles at fluid interfaces via capillarity using a magnetic micro-robot**. *Appl Phys Lett* 2020, **116**, 043702, https://doi.org/10.1063/1.5130635. http://aip.scitation.org/doi/10.1063/1.5130635.
* A microrobot is designed with high curvature as docking sites to induce assembly of passive colloids via capillary interactions. The role of hydrodynamic interactions between active-passive particles is also discussed

24. Pieranski P: **Two-dimensional interfacial colloidal crystals**. *Phys Rev Lett* 1980, **45**:569–572, https://doi.org/10.1103/PhysRevLett.45.569. https://link.aps.org/doi/10.1103/PhysRevLett.45.569.

25. Singh P, Joseph DD, Gurupatham SK, Dalal B, Nudurupati S: **Spontaneous dispersion of particles on liquid surfaces**. *Proc Natl Acad Sci USA* 2009, **106**:19761–19764, https://doi.org/10.1073/pnas.0910343106. https://pnas.org/doi/full/10.1073/pnas.0910343106.

26. Chen L, Heim L-O, Golovko DS, Bonaccurso E: **Snap-in dynamics of single particles to water drops**. *Appl Phys Lett* 2012, **101**, 031601, https://doi.org/10.1063/1.4737210. http://aip.scitation.org/doi/10.1063/1.4737210.

27. Kaz DM, McGorty R, Mani M, Brenner MP, Manoharan VN: **Physical ageing of the contact line on colloidal particles at liquid interfaces**. *Nat Mater* 2012, **11**:138–142, https://doi.org/10.1038/nmat3190. http://www.nature.com/articles/nmat3190.

28. Wang A, McGorty R, Kaz DM, Manoharan VN: **Contact-line pinning controls how quickly colloidal particles equilibrate with liquid interfaces**. *Soft Matter* 2016, **12**:8958–8967, https://doi.org/10.1039/C6SM01690A. http://xlink.rsc.org/?DOI=C6SM01690A.

29. Colosqui CE, Morris JF, Koplik J: **Colloidal adsorption at fluid interfaces: regime crossover from fast relaxation to physical aging**. *Phys Rev Lett* 2013, **111**, 028302, https://doi.org/10.1103/PhysRevLett.111.028302. https://link.aps.org/doi/10.1103/PhysRevLett.111.028302.

30. Blake T, Haynes J: **Kinetics of displacement**. *J Colloid Interface Sci* 1969, **30**:421–423, https://doi.org/10.1016/0021-9797(69)90411-1.

31. Stocco A, Chollet B, Wang X, Blanc C, Nobili M: **Rotational diffusion of partially wetted colloids at fluid interfaces**. *J Colloid Interface Sci* 2019, **542**:363–369, https://doi.org/10.1016/j.jcis.2019.02.017. https://linkinghub.elsevier.com/retrieve/pii/S0021979719301821.
* The reduced rotational diffusivity of partially wetted Janus particles is observed and is explained by the contact line frictions

32. Stamou D, Duschl C, Johannsmann D: **Long-range attraction between colloidal spheres at the air-water interface: the consequence of an irregular meniscus**. *Phys Rev* 2000, **62**:5263–5272, https://doi.org/10.1103/PhysRevE.62.5263. https://link.aps.org/doi/10.1103/PhysRevE.62.5263.

33. Liu IB, Sharifi-Mood N, Stebe KJ: **Capillary assembly of colloids: interactions on planar and curved interfaces**. *Annu Rev Condens Matter Phys* 2018, **9**:283–305, https://doi.org/10.1146/annurev-conmatphys-031016-025514. https://www.annualreviews.org/doi/10.1146/annurev-conmatphys-031016-025514.

34. Manikantan H, Squires TM: **Surfactant dynamics: hidden variables controlling fluid flows**. *J Fluid Mech* 2020, **892**, https://doi.org/10.1017/jfm.2020.170. P1.
** A complete review of transport dynamics of surfactants and their role in interfacial stress boundary conditions. Specifically, they discussed paradigmatic problems from fluid mechanics that are impacted by surfactants and some of the ambiguities

35. Dani A, Keiser G, Yeganeh M, Maldarelli C: **Hydrodynamics of particles at an oil–water interface**. *Langmuir* 2015, **31**:

13290–13302, https://doi.org/10.1021/acs.langmuir.5b02146. https://pubs.acs.org/doi/10.1021/acs.langmuir.5b02146.

36. Blawzdziewicz J, Wajnryb E, Loewenberg M: **Hydrodynamic interactions and collision efficiencies of spherical drops covered with an incompressible surfactant film**. *J Fluid Mech* 1999, **395**:29–59, https://doi.org/10.1017/S002211209900590X.

37. Bławzdziewicz J, Ekiel-Jeżewska ML, Wajnryb E: **Motion of a spherical particle near a planar fluid-fluid interface: the effect of surface incompressibility**. *J Chem Phys* 2010, **133**, 114702, https://doi.org/10.1063/1.3475197.

38. Fischer TM, Dhar P, Heinig P: **The viscous drag of spheres and filaments moving in membranes or monolayers**. *J Fluid Mech* 2006, **558**:451, https://doi.org/10.1017/S002211200600022X.

39. Lopez D, Lauga E: **Dynamics of swimming bacteria at complex interfaces**. *Phys Fluids* 2014, **26**, 071902, https://doi.org/10.1063/1.4887255. http://aip.scitation.org/doi/10.1063/1.4887255.

40. ** Chisholm NG, Stebe KJ: **Driven and active colloids at fluid interfaces**. *J Fluid Mech* 2021, **914**:A29, https://doi.org/10.1017/jfm.2020.708.
The authors derived multipole expressions for planar "clean" and incompressible interfaces. They further discussed the leading-order far-field flows generated by externally driven and self-propelled colloids in these two regimes.

41. ** Molaei M, Chisholm NG, Deng J, Crocker JC, Stebe KJ: **Interfacial flow around brownian colloids**. *Phys Rev Lett* 2021, **126**, 228003, https://doi.org/10.1103/PhysRevLett.126.228003. https://link.aps.org/doi/10.1103/PhysRevLett.126.228003.
The interfacial flow around Brownian particles is visualised using correlated displacement velocimetry. The pronounced effect of trace surfactant contamination renders the interface incompressible. The flow structure indicates interfacial incompressibility and surface viscosity.

42. ** Pourali M, Kröger M, Vermant J, Anderson PD, Jaensson NO: **Drag on a spherical particle at the air–liquid interface: interplay between compressibility, Marangoni flow, and surface viscosities**. *Phys Fluids* 2021, **33**, 062103, https://doi.org/10.1063/5.0050936. https://aip.scitation.org/doi/10.1063/5.0050936.
Using finite element simulations, the authors revealed the coupling between bulk flows and interfaces. They studied the effect of interfacial incompressbility and surface viscosity on the drag coefficient trapped at air–water interfaces.

43. * Das S, Koplik J, Somasundaran P, Maldarelli C: **Pairwise hydrodynamic interactions of spherical colloids at a gas-liquid interface**. *J Fluid Mech* 2021, **915**:A99, https://doi.org/10.1017/jfm.2021.170.
The authors studied the pairwise hydrodynamic interactions between two colloids trapped at the interfaces using finite element simulations. Four different colloidal motions were considered, and the corresponding drag coefficients are calculated.

44. ** Maldarelli C, Donovan NT, Ganesh SC, Das S, Koplik J: **Continuum and molecular dynamics studies of the hydrodynamics of colloids straddling a fluid interface**. *Annu Rev Fluid Mech* 2022, **54**:495–523, https://doi.org/10.1146/annurev-fluid-032621-043917. https://www.annualreviews.org/doi/10.1146/annurev-fluid-032621-043917.
A complete review considering near-field effects of particles on hydrodynamics and drag coefficient of particles at fluid interfaces using finite element simulations and molecular simulations.

45. * Das D, Lauga E: **Transition to bound states for bacteria swimming near surfaces**. *Phys Rev* 2019, **100**, 043117, https://doi.org/10.1103/PhysRevE.100.043117. https://link.aps.org/doi/10.1103/PhysRevE.100.043117.
The authors studied the bound state of bacteria *Thiovulum majas* using numerical simulations and theoretical analysis. They demonstrated that the stability of the bound state depends on the cell morphology.

46. Stone HA, Masoud H: **Mobility of membrane-trapped particles**. *J Fluid Mech* 2015, **781**:494–505, https://doi.org/10.1017/jfm.2015.486.

47. ** Villa S, Boniello G, Stocco A, Nobili M: **Motion of micro- and nano- particles interacting with a fluid interface**. *Adv Colloid Interface Sci* 2020, **284**, 102262, https://doi.org/10.1016/j.cis.2020.102262. https://linkinghub.elsevier.com/retrieve/pii/S000186862030107X.
A recent review paper on the theoretical models and experimental results of the translational and rotational drag of micro-and nanoparticles adjacent to and trapped at fluid interfaces.

48. Boneva MP, Christov NC, Danov KD, Kralchevsky PA: **Effect of electric-field-induced capillary attraction on the motion of particles at an oil–water interface**. *Phys Chem Chem Phys* 2007, **9**:6371, https://doi.org/10.1039/b709123k.

49. Danov K, Aust R, Durst F, Lange U: **Influence of the surface viscosity on the hydrodynamic resistance and surface diffusivity of a large brownian particle**. *J Colloid Interface Sci* 1995, **175**:36–45, https://doi.org/10.1006/jcis.1995.1426. https://linkinghub.elsevier.com/retrieve/pii/S0021979785714269.

50. Danov KD, Dimova R, Pouligny B: **Viscous drag of a solid sphere straddling a spherical or flat surface**. *Phys Fluids* 2000, **12**:2711, https://doi.org/10.1063/1.1289692. http://scitation.aip.org/content/aip/journal/pof2/12/11/10.1063/1.1289692.

51. Pozrikidis C: **Particle motion near and inside an interface**. *J Fluid Mech* 2007, **575**:333–357, https://doi.org/10.1017/S0022112006004046.

52. Dörr A, Hardt S, Masoud H, Stone HA: **Drag and diffusion coefficients of a spherical particle attached to a fluid–fluid interface**. *J Fluid Mech* 2016, **790**:607–618, https://doi.org/10.1017/jfm.2016.41.

53. Koplik J, Maldarelli C: **Diffusivity and hydrodynamic drag of nanoparticles at a vapor-liquid interface**. *Phys Rev Fluids* 2017, **2**, 024303, https://doi.org/10.1103/PhysRevFluids.2.024303. https://link.aps.org/doi/10.1103/PhysRevFluids.2.024303.

54. Boniello G, Blanc C, Fedorenko D, Medfai M, Mbarek NB, In M, Gross M, Stocco A, Nobili M: **Brownian diffusion of a partially wetted colloid**. *Nat Mater* 2015, **14**:908–911, https://doi.org/10.1038/nmat4348.

55. Saffman PG, Delbrück M: **Brownian motion in biological membranes**. *Proc Natl Acad Sci USA* 1975, **72**:3111–3113, https://doi.org/10.1073/pnas.72.8.3111. https://pnas.org/doi/full/10.1073/pnas.72.8.3111.

56. Fischer TM: **The drag on needles moving in a Langmuir monolayer**. *J Fluid Mech* 2004, **498**:123–137, https://doi.org/10.1017/S0022112003006608.

57. Stone HA, Ajdari A: **Hydrodynamics of particles embedded in a flat surfactant layer overlying a subphase of finite depth**. *J Fluid Mech* 1998, **369**:151–173, https://doi.org/10.1017/S0022112098001980.

58. Levine AJ, MacKintosh FC: **Dynamics of viscoelastic membranes**. *Phys Rev* 2002, **66**, 061606, https://doi.org/10.1103/PhysRevE.66.061606. https://link.aps.org/doi/10.1103/PhysRevE.66.061606.

59. Kim K, Choi SQ, Zasadzinski JA, Squires TM: **Interfacial microrheology of DPPC monolayers at the air–water interface**. *Soft Matter* 2011, **7**:7782, https://doi.org/10.1039/c1sm05383c. http://xlink.rsc.org/?DOI=c1sm05383c.

60. Lee MH, Lapointe CP, Reich DH, Stebe KJ, Leheny RL: **Interfacial hydrodynamic drag on nanowires embedded in thin oil films and protein layers**. *Langmuir* 2009, **25**:7976–7982, https://doi.org/10.1021/la900408y. https://pubs.acs.org/doi/10.1021/la900408y.

61. * Chang C-C, Nowbahar A, Mansard V, Williams I, Mecca J, Schmitt AK, Kalantar TH, Kuo T-C, Squires TM: **Interfacial rheology and heterogeneity of aging asphaltene layers at the water–oil interface**. *Langmuir* 2018, **34**:5409–5415, https://doi.org/10.1021/acs.langmuir.8b00176. https://pubs.acs.org/doi/10.1021/acs.langmuir.8b00176.
The authors used ferromagnetic microbuttons driven by a sinusoidal magnetic field to study the rheology of aging asphaltene layers. The amplitude of the induced displacement and its phase lag relative to the driving field are measured to determine the complex drag resistance of the particles and subsequently complex viscosity of the interface.

62. Kim K, Choi SQ, Zasadzinski JA, Squires TM: **Nonlinear chiral rheology of phospholipid monolayers**. *Soft Matter* 2018, **14**:

2476–2483, https://doi.org/10.1039/C8SM00184G. http://xlink.rsc.org/?DOI=C8SM00184G.

63. * Williams I, Zasadzinski JA, Squires TM: **Interfacial rheology and direct imaging reveal domain-templated network formation in phospholipid monolayers penetrated by fibrinogen**. *Soft Matter* 2019, **15**:9076–9084, https://doi.org/10.1039/C9SM01519A. http://xlink.rsc.org/?DOI=C9SM01519A.
The author studied the interfacial rheology and domain formation in phosopholipid monolayer penetrated by fibrinogen. The magnetic microbutton under a sinusoidal field is used to quantify the interfacial shear response. Confocal and epifluorescence microscopy are used for imaging the morphological evolution.

64. Manneville J-B, Bassereau P, Lévy D, Prost J: **Activity of transmembrane proteins induces magnification of shape fluctuations of lipid membranes**. *Phys Rev Lett* 1999, **82**:4356–4359, https://doi.org/10.1103/PhysRevLett.82.4356. https://link.aps.org/doi/10.1103/PhysRevLett.82.4356.

65. Huang M-J, Kapral R, Mikhailov AS, Chen H-Y: **Coarse-grain simulations of active molecular machines in lipid bilayers**. *J Chem Phys* 2013, **138**, 195101, https://doi.org/10.1063/1.4803507. http://aip.scitation.org/doi/10.1063/1.4803507.

66. Hosaka Y, Yasuda K, Okamoto R, Komura S: **Lateral diffusion induced by active proteins in a biomembrane**. *Phys Rev* 2017, **95**, 052407, https://doi.org/10.1103/PhysRevE.95.052407. http://link.aps.org/doi/10.1103/PhysRevE.95.052407.

67. ** Manikantan H: **Tunable collective dynamics of active inclusions in viscous membranes**. *Phys Rev Lett* 2020, **125**, 268101, https://doi.org/10.1103/PhysRevLett.125.268101. https://link.aps.org/doi/10.1103/PhysRevLett.125.268101.
The authors developed a theoretical framework to study the hydrodynamic interaction and clustering mechanisms of these active membrane inclusions.

68. Elfring GJ, Leal LG, Squires TM: **Surface viscosity and Marangoni stresses at surfactant laden interfaces**. *J Fluid Mech* 2016, **792**:712–739, https://doi.org/10.1017/jfm.2016.96.

69. Zell ZA, Nowbahar A, Mansard V, Leal LG, Deshmukh SS, Mecca JM, Tucker CJ, Squires TM: **Surface shear inviscidity of soluble surfactants**. *Proc Natl Acad Sci USA* 2014, **111**:3677–3682, https://doi.org/10.1073/pnas.1315991111. https://pnas.org/doi/full/10.1073/pnas.1315991111.

70. Drescher K, Dunkel J, Cisneros LH, Ganguly S, Goldstein RE: **Fluid dynamics and noise in bacterial cell–cell and cell–surface scattering**. *Proc Natl Acad Sci USA* 2011, **108**:10940–10945, https://doi.org/10.1073/pnas.1019079108. https://pnas.org/doi/full/10.1073/pnas.1019079108.

71. Drescher K, Goldstein RE, Michel N, Polin M, Tuval I: **Direct measurement of the flow field around swimming microorganisms**. *Phys Rev Lett* 2010, **105**, 168101, https://doi.org/10.1103/PhysRevLett.105.168101. https://link.aps.org/doi/10.1103/PhysRevLett.105.168101.

72. Lemelle L, Palierne J-F, Chatre E, Place C: **Counterclockwise circular motion of bacteria swimming at the air-liquid interface**. *J Bacteriol* 2010, **192**:6307–6308, https://doi.org/10.1128/JB.00397-10. https://journals.asm.org/doi/10.1128/JB.00397-10.

73. Morse M, Huang A, Li G, Maxey M, Tang J: **Molecular adsorption steers bacterial swimming at the air/water interface**. *Biophys J* 2013, **105**:21–28, https://doi.org/10.1016/j.bpj.2013.05.026. https://linkinghub.elsevier.com/retrieve/pii/S0006349513005833.

74. Camilli R, Reddy CM, Yoerger DR, Van Mooy BAS, Jakuba MV, Kinsey JC, McIntyre CP, Sylva SP, Maloney JV: **Tracking hydrocarbon plume transport and biodegradation at deepwater Horizon**. *Science* 2010, **330**:201–204, https://doi.org/10.1126/science.1195223.

75. Hazen TC, Dubinsky EA, DeSantis TZ, Andersen GL, Piceno YM, Singh N, Jansson JK, Probst A, Borglin SE, Fortney JL, Stringfellow WT, Bill M, Conrad ME, Tom LM, Chavarria KL, Alusi TR, Lamendella R, Joyner DC, Spier C, Baelum J, Auer M, Zemla ML, Chakraborty R, Sonnenthal EL, D'haeseleer P, Holman H-YN, Osman S, Lu Z, Van Nostrand JD, Deng Y, Zhou J, Mason OU: **Deep-Sea oil plume enriches indigenous oil-degrading bacteria**. *Science* 2010, **330**:204–208, https://doi.org/10.1126/science.1195979. https://www.science.org/doi/10.1126/science.1195979.

76. Atlas RM, Hazen TC: **Oil biodegradation and bioremediation: a tale of the two worst spills in U.S. History**. *Environ Sci Technol* 2011, **45**:6709–6715, https://doi.org/10.1021/es2013227.

77. * Desai N, Shaik VA, Ardekani AM: **Hydrodynamics-mediated trapping of micro-swimmers near drops**. *Soft Matter* 2018, **14**:264–278, https://doi.org/10.1039/C7SM01615H. http://xlink.rsc.org/?DOI=C7SM01615H.
Using theoretical model on force dipole near fluid interfaces, the authors calculate hydrodynamic component velocity and rotational velocity of bacteria near the droplets. They found bacteria can be hydrodynamically trapped near interfaces at critical trapping radius or scattered away due to steric repulsion and Brownian diffusivity of swimmers.

78. * Ahmadzadegan A, Wang S, Vlachos PP, Ardekani AM: **Hydrodynamic attraction of bacteria to gas and liquid interfaces**. *Phys Rev* 2019, **100**, 062605, https://doi.org/10.1103/PhysRevE.100.062605.
Using higher-order hydrodynamic singularies generated by bacteria near the interfaces, these authors explained the experimentally observed tilted angle of bacteria and their strong accumulation near air–water interfaces.

79. * Bianchi S, Saglimbeni F, Frangipane G, Dell'Arciprete D, Di Leonardo R: **3D dynamics of bacteria wall entrapment at a water–air interface**. *Soft Matter* 2019, **15**:3397–3406, https://doi.org/10.1039/C9SM00077A.
An experimental study on bacteria's motion near air-liquid interfaces, where the authors observed a tilted angle of bacteria similar to their orientations near the solid surfaces.

80. ** Liebchen B, Monderkamp P, ten Hagen B, Löwen H: ***Viscotaxis*: microswimmer navigation in viscosity gradients**. *Phys Rev Lett* 2018, **120**, 208002, https://doi.org/10.1103/PhysRevLett.120.208002. https://link.aps.org/doi/10.1103/PhysRevLett.120.208002.
Modeling the swimmers with assemblies of spheres, the authors showed that the nonuniaxial body shapes of swimmers automatically lead to viscous torques that align the swimmers generically up viscosity gradients.

81. ** Datt C, Elfring GJ: **Active particles in viscosity gradients**. *Phys Rev Lett* 2019, **123**, 158006, https://doi.org/10.1103/PhysRevLett.123.158006. https://link.aps.org/doi/10.1103/PhysRevLett.123.158006.
The authors used axisymmetric squirmers to model pusher and puller swimmers, and showed that uniaxial swimmers can display negative viscotaxis for all types of swimmers due to the effect of viscosity gradient on thrust generated by the swimming gait.

82. ** Stehnach MR, Waisbord N, Walkama DM, Guasto JS: **Viscophobic turning dictates microalgae transport in viscosity gradients**. *Nat Phys* 2021, **17**:926–930, https://doi.org/10.1038/s41567-021-01247-7. https://www.nature.com/articles/s41567-021-01247-7.
The authors observed the viscophobic mobility of puller swimmer, *Chlamydomonas reinhardtii*. Flagellar thrust imbalance slows down the swimmer and reorients swimmers down the viscosity gradient resulting in strong accumulation in low-viscosity region.

83. ** Coppola S, Kantsler V: **Green algae scatter off sharp viscosity gradients**. *Sci Rep* 2021, **11**:399, https://doi.org/10.1038/s41598-020-79887-7. http://www.nature.com/articles/s41598-020-79887-7.
The authors performed experiments with puller microswimmer and showed that that the velocity and angular diffusion of the algae decreases when the viscosity of the surrounding medium is increased. Scattering occurs when algae cross the sharp viscosity gradient.

84. * Lopez CE, Gonzalez-Gutierrez J, Solorio-Ordaz F, Lauga E, Zenit R: **Dynamics of a helical swimmer crossing viscosity gradients**. *Phys Rev Fluids* 2021, **6**, 083102, https://doi.org/10.1103/PhysRevFluids.6.083102. http://arxiv.org/abs/2012.04788.
The authors studied the behavior of helical swimmers across the viscosity gradients using synthetic helical magnetic driven swimmers. For "pusher" swimmers, the swimmer's head crosses the viscosity gradient followed by its tail which leads to the changes in drag and subsequently propulsion. Opposite changes in drag and propulsion force are experienced by puller (tail first) swimmer, which lead to different swimming behaviors.

85. * Eastham PS, Shoele K: **Axisymmetric squirmers in Stokes fluid with nonuniform viscosity**. *Phys Rev Fluids* 2020, **5**, 063102, https://doi.org/10.1103/PhysRevFluids.5.063102. https://link.aps.org/doi/10.1103/PhysRevFluids.5.063102.
Using an axisymmetric squirmer model, the authors studied the response of swimmers due to the coupling effect of nutrient and viscosity gradients.

86. McLay RB, Nguyen HN, Jaimes-Lizcano YA, Dewangan NK, Alexandrova S, Rodrigues DF, Cirino PC, Conrad JC: **Level of fimbriation alters the adhesion of *Escherichia coli* bacteria to interfaces**. *Langmuir* 2018, **34**:1133–1142, https://doi.org/10.1021/acs.langmuir.7b02447. https://pubs.acs.org/doi/10.1021/acs.langmuir.7b02447.

87. Dewangan NK, Conrad JC: **Adhesion of *Marinobacter hydrocarbonoclasticus* to surfactant-decorated dodecane droplets**. *Langmuir* 2018, **34**:14012–14021, https://doi.org/10.1021/acs.langmuir.8b02071. https://pubs.acs.org/doi/10.1021/acs.langmuir.8b02071.

88. * Dewangan NK, Conrad JC: **Bacterial motility enhances adhesion to oil droplets**. *Soft Matter* 2020, **16**:8237–8244, https://doi.org/10.1039/D0SM00944J. http://xlink.rsc.org/?DOI=D0SM00944J.
The authors used a proton uncoupler to showed that motility of *Halomonas titanicae* can enhance their adhesion to oil droplets.

89. * Dewangan NK, Conrad JC: **Rotating oil droplets driven by motile bacteria at interfaces**. *Soft Matter* 2019, **15**:9368–9375, https://doi.org/10.1039/C9SM01570A. http://xlink.rsc.org/?DOI=C9SM01570A.
Adhered bacteria at the surface of oil droplets can drive their rotations near solid surfaces. Such adhesion can be reduced by adding surfactants to the system.

90. Niepa THR, Vaccari L, Leheny RL, Goulian M, Lee D, Stebe KJ: **Films of bacteria at interfaces (FBI): remodeling of fluid interfaces by Pseudomonas aeruginosa**. *Sci Rep* 2017, **7**, 17864, https://doi.org/10.1038/s41598-017-17721-3. http://www.nature.com/articles/s41598-017-17721-3.

91. Vaccari L, Allan DB, Sharifi-Mood N, Singh AR, Leheny RL, Stebe KJ: **Films of bacteria at interfaces: three stages of behaviour**. *Soft Matter* 2015, **11**:6062–6074, https://doi.org/10.1039/C5SM00696A. http://xlink.rsc.org/?DOI=C5SM00696A.

92. Vaccari L, Molaei M, Niepa TH, Lee D, Leheny RL, Stebe KJ: **Films of bacteria at interfaces**. *Adv Colloid Interface Sci* 2017, **247**:561–572, https://doi.org/10.1016/j.cis.2017.07.016. https://linkinghub.elsevier.com/retrieve/pii/S0001868617302373.

93. Qi L, Christopher GF: **Role of flagella, type IV pili, biosurfactants, and extracellular polymeric substance polysaccharides on the formation of pellicles by *Pseudomonas aeruginosa***. *Langmuir* 2019, **35**:5294–5304, https://doi.org/10.1021/acs.langmuir.9b00271. https://pubs.acs.org/doi/10.1021/acs.langmuir.9b00271.

94. * Balmuri SR, Phandanouvong-Lozano V, House SD, Yang JC, Niepa TH: **Mucoid coating provides a growth advantage to *Pseudomonas aeruginosa* at oil–water interfaces**. *ACS Appl Bio Mater* 2022, **5**:1868–1878, https://doi.org/10.1021/acsabm.1c01198.
The authors studied the phenotypical change of *P. aeruginosa* trapped at fluid interfaces. They found bacteria switch to mucoid cells to protect themselves from interfacial stresses.

95. White AR, Jalali M, Sheng J: **A new ecology-on-a-chip microfluidic platform to study interactions of microbes with a rising oil droplet**. *Sci Rep* 2019, **9**, 13737, https://doi.org/10.1038/s41598-019-50153-9. http://www.nature.com/articles/s41598-019-50153-9.

96. * White AR, Jalali M, Boufadel MC, Sheng J: **Bacteria forming drag-increasing streamers on a drop implicates complementary fates of rising deep-sea oil droplets**. *Sci Rep* 2020, **10**:4305, https://doi.org/10.1038/s41598-020-61214-9. http://www.nature.com/articles/s41598-020-61214-9.
Using microfluidics platforms, the authors studied bacteria-oil droplet interactions under flowing conditions, where they found bacterial Extracellular Polymeric Substances (EPS) threads developed behind the droplets can slow down the rising droplets.

97. Deng J, Molaei M, Chisholm NG, Stebe KJ: ***Interfacial flow around a pusher bacterium***. Technical Report arXiv: 2204.02300, arXiv, http://arxiv.org/abs/2204.02300. arXiv: 2204.02300 [physics] type: article.

98. Ishimoto K: **Bacterial spinning top**. *J Fluid Mech* 2019, **880**: 620–652, https://doi.org/10.1017/jfm.2019.714.

99. de Anda J, Lee EY, Lee CK, Bennett RR, Ji X, Soltani S, Harrison MC, Baker AE, Luo Y, Chou T, O'Toole GA, Armani AM, Golestanian R, Wong GCL: **High-speed "4D" computational microscopy of bacterial surface motility**. *ACS Nano* 2017, **11**: 9340–9351, https://doi.org/10.1021/acsnano.7b04738. https://pubs.acs.org/doi/10.1021/acsnano.7b04738.

100. Kühn MJ, Schmidt FK, Eckhardt B, Thormann KM: **Bacteria exploit a polymorphic instability of the flagellar filament to escape from traps**. *Proc Natl Acad Sci USA* 2017, **114**: 6340–6345, https://doi.org/10.1073/pnas.1701644114. https://pnas.org/doi/full/10.1073/pnas.1701644114.

101. Hintsche M, Waljor V, Großmann R, Kühn MJ, Thormann KM, Peruani F, Beta C: **A polar bundle of flagella can drive bacterial swimming by pushing, pulling, or coiling around the cell body**. *Sci Rep* 2017, **7**, 16771, https://doi.org/10.1038/s41598-017-16428-9. http://www.nature.com/articles/s41598-017-16428-9.

102. Constantino MA, Jabbarzadeh M, Fu HC, Shen Z, Fox JG, Haesebrouck F, Linden SK, Bansil R: **Bipolar lophotrichous Helicobacter suis combine extended and wrapped flagella bundles to exhibit multiple modes of motility**. *Sci Rep* 2018, **8**, 14415, https://doi.org/10.1038/s41598-018-32686-7. http://www.nature.com/articles/s41598-018-32686-7.

103. Molaei M, Barry M, Stocker R, Sheng J: **Failed escape: solid surfaces prevent tumbling of <i>Escherichia coli<\i&gt**. *Phys Rev Lett* 2014, **113**, https://doi.org/10.1103/PhysRevLett.113.068103. https://link.aps.org/doi/10.1103/PhysRevLett.113.068103.

104. Gidituri H, Shen Z, Wurger A, Lintuvuori JS: **Reorientation dynamics of microswimmers at fluid-fluid interfaces**. *Phys Rev Fluids* 2022, **7**:L042001, https://doi.org/10.1103/PhysRevFluids.7.L042001. arXiv:2202.10421 [cond-mat, physics:physics], http://arxiv.org/abs/2202.10421.

105. Son K, Guasto JS, Stocker R: **Bacteria can exploit a flagellar buckling instability to change direction**. *Nat Phys* 2013, **9**: 494–498, https://doi.org/10.1038/nphys2676. http://www.nature.com/articles/nphys2676.

106. Nguyen FTM, Graham MD: **Impacts of multiflagellarity on stability and speed of bacterial locomotion**. *Phys Rev* 2018, **98**, 042419, https://doi.org/10.1103/PhysRevE.98.042419. https://link.aps.org/doi/10.1103/PhysRevE.98.042419.

107. Zhang W-J, Wu L-F: **Flagella and swimming behavior of marine magnetotactic bacteria**. *Biomolecules* 2020, **10**:460, https://doi.org/10.3390/biom10030460. https://www.mdpi.com/2218-273X/10/3/460.

108. * Palacios LS, Katuri J, Pagonabarraga I, Sánchez S: **Guidance of active particles at liquid–liquid interfaces near surfaces**. *Soft Matter* 2019, **15**:6581–6588, https://doi.org/10.1039/C9SM01016E. http://xlink.rsc.org/?DOI=C9SM01016E.
Active Janus particles tend to reorient parallel to the interfaces, and slide near the interfaces. Similar behaviors are observed near the three-phase contact line of a sessile droplet.

109. * Wittmann M, Popescu MN, Domínguez A, Simmchen J: **Active spheres induce Marangoni flows that drive collective dynamics**. *Eur Phys J C* 2021, **44**:15, https://doi.org/10.1140/epje/s10189-020-00006-5. https://link.springer.com/10.1140/epje/s10189-020-00006-5.
Marangoni flow break the radial symmetry of isotropic chemically active particles with the presence of neighboring particles and induce collective behaviors.

110. * Dietrich K, Renggli D, Zanini M, Volpe G, Buttinoni I, Isa L: **Two-dimensional nature of the active Brownian motion of catalytic microswimmers at solid and liquid interfaces**. *New J Phys* 2017, **19**, 065008, https://doi.org/10.1088/1367-2630/aa7126. https://iopscience.iop.org/article/10.1088/1367-2630/aa7126.
The authors observed various trapping configurations of Janus particles and related their trapping to the propulsive speed and rotational diffusivities.

111. Howse JR, Jones RAL, Ryan AJ, Gough T, Vafabakhsh R, Golestanian R: **Self-motile colloidal particles: from directed propulsion to random walk**. *Phys Rev Lett* 2007, **99**, 048102, https://doi.org/10.1103/PhysRevLett.99.048102. https://link.aps.org/doi/10.1103/PhysRevLett.99.048102.

112. Paxton WF, Kistler KC, Olmeda CC, Sen A, Angelo S K St, Cao Y, Mallouk TE, Lammert PE, Crespi VH: **Catalytic nanomotors: autonomous movement of striped nanorods**. *J Am Chem Soc* 2004, **126**:13424–13431, https://doi.org/10.1021/ja047697z. https://pubs.acs.org/doi/10.1021/ja047697z.

113. ** Campbell AI, Ebbens SJ, Illien P, Golestanian R: **Experimental observation of flow fields around active Janus spheres**. *Nat Commun* 2019, **10**:3952, https://doi.org/10.1038/s41467-019-11842-1.
Flow field around a free-swimming Janus particle and a Janus particle stuck at the wall was observed and understood theoretically. The far-field flow around the Janus particle can be described as a force dipole with a complex near-field structure due to phoretic effect.

114. Spagnolie SE, Lauga E: **Hydrodynamics of self-propulsion near a boundary: predictions and accuracy of far-field approximations**. *J Fluid Mech* 2012, **700**:105–147, https://doi.org/10.1017/jfm.2012.101.

115. Jalilvand Z, Haider H, Cui J, Kretzschmar aI: **Pt-SiO $_2$ Janus particles and the water/oil interface: a competition between motility and thermodynamics**. *Langmuir* 2020, **36**:6880–6887, https://doi.org/10.1021/acs.langmuir.9b03454. https://pubs.acs.org/doi/10.1021/acs.langmuir.9b03454.

116. Wang W, Giltinan J, Zakharchenko S, Sitti M: **Dynamic and programmable self-assembly of micro-rafts at the air-water interface**. *Sci Adv* 2017, **3**, e1602522, https://doi.org/10.1126/sciadv.1602522. https://www.science.org/doi/10.1126/sciadv.1602522.

117. Kümmel F, ten Hagen B, Wittkowski R, Buttinoni I, Eichhorn R, Volpe G, Löwen H, Bechinger C: **Circular motion of asymmetric self-propelling particles**. *Phys Rev Lett* 2013, **110**, 198302, https://doi.org/10.1103/PhysRevLett.110.198302. https://link.aps.org/doi/10.1103/PhysRevLett.110.198302.

118. Malgaretti P, Popescu MN, Dietrich S: **Active colloids at fluid interfaces**. *Soft Matter* 2016, **12**:4007–4023, https://doi.org/10.1039/C6SM00367B. http://xlink.rsc.org/?DOI=C6SM00367B.

119. * Peter T, Malgaretti P, Rivas N, Scagliarini A, Harting J, Dietrich S: **Numerical simulations of self-diffusiophoretic colloids at fluid interfaces**. *Soft Matter* 2020, **16**:3536–3547, https://doi.org/10.1039/C9SM02247C. http://xlink.rsc.org/?DOI=C9SM02247C.
Using a mesoscopic numerical approach, the author showed that when adsorbed at a fluid interface, an active colloid experiences a net torque even in the absence of a viscosity contrast between the two adjacent fluids. This torque is caused by non-homogeneous mobility along the surface of the colloids.

120. Wang X, In M, Blanc C, Nobili M, Stocco A: **Enhanced active motion of Janus colloids at the water surface**. *Soft Matter* 2015, **11**:7376–7384, https://doi.org/10.1039/C5SM01111F. http://xlink.rsc.org/?DOI=C5SM01111F.

121. Simmchen J, Katuri J, Uspal WE, Popescu MN, Tasinkevych M, Sánchez S: **Topographical pathways guide chemical microswimmers**. *Nat Commun* 2016, **7**, 10598, https://doi.org/10.1038/ncomms10598. http://www.nature.com/articles/ncomms10598.

122. Popescu MN, Uspal WE, Dietrich S: **Self-diffusiophoresis of chemically active colloids**. *Eur Phys J Spec Top* 2016, **225**:2189–2206, https://doi.org/10.1140/epjst/e2016-60058-2. http://link.springer.com/10.1140/epjst/e2016-60058-2.

123. * Popescu MN, Uspal WE, Domínguez A, Dietrich S: **Effective interactions between chemically active colloids and interfaces**. *Accounts Chem Res* 2018, **51**:2991–2997, https://doi.org/10.1021/acs.accounts.8b00237. https://pubs.acs.org/doi/10.1021/acs.accounts.8b00237.
A short review on the complex behaviors of chemically active colloids near different boundaries, and how to understand them via chemical activity and phoretic interactions.

124. Sharan P, Postek W, Gemming T, Garstecki P, Simmchen J: **Study of active Janus particles in the presence of an engineered oil–water interface**. *Langmuir* 2021, **37**:204–210, https://doi.org/10.1021/acs.langmuir.0c02752. https://pubs.acs.org/doi/10.1021/acs.langmuir.0c02752.

125. Malgaretti P, Popescu MN, Dietrich S: **Self-diffusiophoresis induced by fluid interfaces**. *Soft Matter* 2018, **14**:1375–1388, https://doi.org/10.1039/C7SM02347B. http://xlink.rsc.org/?DOI=C7SM02347B.

126. Domínguez A, Malgaretti P, Popescu M, Dietrich S: **Effective interaction between active colloids and fluid interfaces induced by Marangoni flows**. *Phys Rev Lett* 2016, **116**, 078301, https://doi.org/10.1103/PhysRevLett.116.078301. https://link.aps.org/doi/10.1103/PhysRevLett.116.078301.

127. Daddi-Moussa-Ider A, Vilfan A, Golestanian R: **Diffusiophoretic propulsion of an isotropic active colloidal particle near a finite-sized disk embedded in a planar fluid-fluid interface**. *J Fluid Mech* 2022, **940**:A12, https://doi.org/10.1017/jfm.2022.232. arXiv:2109.14437 [cond-mat, physics:physics].

128. ** Correia EL, Brown N, Razavi S: **Janus particles at fluid interfaces: stability and interfacial rheology**. *Nanomaterials* 2021, **11**:374, https://doi.org/10.3390/nano11020374. https://www.mdpi.com/2079-4991/11/2/374.
A recent review paper on the adsorption dynamics of Janus particles to the fluid interfaces, their trapping states, surface rheology of particle laden interfaces and their applications in the interfacial engineering.

129. Lan Y, Choi J, Li H, Jia Y, Huang R, Stebe KJ, Lee D: **Janus particles with varying configurations for emulsion stabilization**. *Ind Eng Chem Res* 2019, **58**:20961–20968, https://doi.org/10.1021/acs.iecr.9b02697. https://pubs.acs.org/doi/10.1021/acs.iecr.9b02697.

130. Razavi S, Lin B, Lee KYC, Tu RS, Kretzschmar I: **Impact of surface amphiphilicity on the interfacial behavior of Janus particle layers under compression**. *Langmuir* 2019, **35**:15813–15824, https://doi.org/10.1021/acs.langmuir.9b01664. https://pubs.acs.org/doi/10.1021/acs.langmuir.9b01664.

131. Bradley LC, Chen W-H, Stebe KJ, Lee D: **Janus and patchy colloids at fluid interfaces**. *Curr Opin Colloid Interface Sci* 2017, **30**:25–33, https://doi.org/10.1016/j.cocis.2017.05.001.

132. Hossain MT, Gates ID, Natale G: **Dynamics of Brownian Janus rods at a liquid–liquid interface**. *Phys Fluids* 2022, **34**, 012117, https://doi.org/10.1063/5.0076148. https://aip.scitation.org/doi/10.1063/5.0076148.

133. Koplik J, Maldarelli C: **Molecular dynamics study of the translation and rotation of amphiphilic Janus nanoparticles at a vapor-liquid surface**. *Phys Rev Fluids* 2019, **4**, 044201, https://doi.org/10.1103/PhysRevFluids.4.044201. https://link.aps.org/doi/10.1103/PhysRevFluids.4.044201.

134. Bush JW, Hu DL: **Walking on water: biolocomotion at the interface**. *Annu Rev Fluid Mech* 2006, **38**:339–369, https://doi.org/10.1146/annurev.fluid.38.050304.092157.

135. ** Dietrich K, Jaensson N, Buttinoni I, Volpe G, Isa L: **Microscale Marangoni surfers**. *Phys Rev Lett* 2020, **125**, 098001, https://doi.org/10.1103/PhysRevLett.125.098001. https://link.aps.org/doi/10.1103/PhysRevLett.125.098001.
Using laser to induce surface tension gradient, the authors designed a microscale Marangoni surfer with a wide range of propulsive speed. The effect of Peclet number and presence of surfactants on its behaviors is discussed.

136. ** Choi Y, Park C, Lee AC, Bae J, Kim H, Choi H, Song Sw, Jeong Y, Choi J, Lee H, Kwon S, Park W: **Photopatterned microswimmers with programmable motion without external stimuli**. *Nat Commun* 2021, **12**:4724, https://doi.org/10.1038/s41467-021-24996-8. https://www.nature.com/articles/s41467-021-24996-8.
Using photopatterning method, the authors designed a Marangoni driven microscale swimmers with controlled release of the chemical fuel to fulfill different swimming trajectories.

137. Okawa D, Pastine SJ, Zettl A, Fréchet JMJ: **Surface tension mediated conversion of light to work**. *J Am Chem Soc* 2009, **131**:5396–5398, https://doi.org/10.1021/ja900130n. https://pubs.acs.org/doi/10.1021/ja900130n.

138. Maggi C, Saglimbeni F, Dipalo M, De Angelis F, Di Leonardo R: **Micromotors with asymmetric shape that efficiently convert light into work by thermocapillary effects**. *Nat Commun* 2015, **6**:7855, https://doi.org/10.1038/ncomms8855. http://www.nature.com/articles/ncomms8855.

139. Song L, Cai J, Zhang S, Liu B, Zhao Y-D, Chen W: **Light-controlled spiky micromotors for efficient capture and transport of targets**. *Sensor Actuator B Chem* 2022, **358**, 131523, https://doi.org/10.1016/j.snb.2022.131523. https://linkinghub.elsevier.com/retrieve/pii/S0925400522001654.

140. Girot A, Danné N, Würger A, Bickel T, Ren F, Loudet JC, Pouligny B: **Motion of optically heated spheres at the water–air interface**. *Langmuir* 2016, **32**:2687–2697, https://doi.org/10.1021/acs.langmuir.6b00181. https://pubs.acs.org/doi/10.1021/acs.langmuir.6b00181.

141. Tiwari I, Parmananda P, Chelakkot R: **Periodic oscillations in a string of camphor infused disks**. *Soft Matter* 2020, **16**:10334–10344, https://doi.org/10.1039/D0SM01393E. http://xlink.rsc.org/?DOI=D0SM01393E.

142. Kitahata H, Koyano Y: **Spontaneous motion of a camphor particle with a triangular modification from a circle**. *J Phys Soc Jpn* 2020, **89**, 094001, https://doi.org/10.7566/JPSJ.89.094001. https://journals.jps.jp/doi/10.7566/JPSJ.89.094001.

143. Koyano Y, Kitahata H: **Imperfect bifurcation in the rotation of a propeller-shaped camphor rotor**. *Phys Rev* 2021, **103**, 012202, https://doi.org/10.1103/PhysRevE.103.012202. https://link.aps.org/doi/10.1103/PhysRevE.103.012202.

144. Akella V, Singh DK, Mandre S, Bandi M: **Dynamics of a camphoric acid boat at the air–water interface**. *Phys Lett* 2018, **382**:1176–1180, https://doi.org/10.1016/j.physleta.2018.02.026.

145. Suematsu NJ, Nakata S: **Evolution of self-propelled objects: from the viewpoint of nonlinear science**. *Chem Eur J* 2018, **24**:6308–6324, https://doi.org/10.1002/chem.201705171. https://onlinelibrary.wiley.com/doi/10.1002/chem.201705171.

146. * Gidituri H, Panchagnula MV, Pototsky A: **Dynamics of a fully wetted Marangoni surfer at the fluid–fluid interface**. *Soft Matter* 2019, **15**:2284–2291, https://doi.org/10.1039/C8SM02102C. http://xlink.rsc.org/?DOI=C8SM02102C.
Using a squirmer model, the authors studied the motion of a fully wetted swimmer and they argued that the motion of isotropic particle may not be persistent at finite *Pe* due to the effect of finite size of particle.

147. Hill RJ, Afuwape G: **Dynamic mobility of surfactant-stabilized nano-drops: unifying equilibrium thermodynamics, electrokinetics and Marangoni effects**. *J Fluid Mech* 2020, **895**:A14, https://doi.org/10.1017/jfm.2020.256.

148. Zavabeti A, Daeneke T, Chrimes AF, O'Mullane AP, Zhen Ou J, Mitchell A, Khoshmanesh K, Kalantar-zadeh K: **Ionic imbalance induced self-propulsion of liquid metals**. *Nat Commun* 2016, **7**, 12402, https://doi.org/10.1038/ncomms12402. http://www.nature.com/articles/ncomms12402.

149. Sur S, Masoud H, Rothstein JP: **Translational and rotational motion of disk-shaped Marangoni surfers**. *Phys Fluids* 2019, **31**, 102101, https://doi.org/10.1063/1.5119360. http://aip.scitation.org/doi/10.1063/1.5119360.

150. ** Jafari Kang S, Sur S, Rothstein JP, Masoud H: **Forward, reverse, and no motion of Marangoni surfers under confinement**. *Phys Rev Fluids* 2020, **5**, 084004, https://doi.org/10.1103/PhysRevFluids.5.084004. https://link.aps.org/doi/10.1103/PhysRevFluids.5.084004.
Using both experimental observations and numerical simulations, the authors studied the motion of Marangoni surfers and their induced flow in the limit of finite Reynolds number and Peclet number. The reverse motion of swimmers is explained by the negative pressure due to strong confinement.

151. Ender H, Kierfeld J: **From diffusive mass transfer in Stokes flow to low Reynolds number Marangoni boats**. *Eur Phys J C* 2021, **44**:4, https://doi.org/10.1140/epje/s10189-021-00034-9. https://link.springer.com/10.1140/epje/s10189-021-00034-9.

152. Ender H, Froin A-K, Rehage H, Kierfeld J: **Surfactant-loaded capsules as Marangoni microswimmers at the air–water interface: symmetry breaking and spontaneous propulsion by surfactant diffusion and advection**. *Eur Phys J C* 2021, **44**:21, https://doi.org/10.1140/epje/s10189-021-00035-8. https://link.springer.com/10.1140/epje/s10189-021-00035-8.

153. * Boniface D, Cottin-Bizonne C, Kervil R, Ybert C, Detcheverry F: **Self-propulsion of symmetric chemically active particles: point-source model and experiments on camphor disks**. *Phys Rev* 2019, **99**, 062605, https://doi.org/10.1103/PhysRevE.99.062605.
Using a point force model, the authors studied the propulsive velocity of Marangoni surfers neglecting the Marangoni flow, and showed that their motion is dominated by advection and has weaker dependence on their intrinsic asymmetry in the high *Pe* regime.

154. * Boniface D, Cottin-Bizonne C, Detcheverry F, Ybert C: **Role of Marangoni forces in the velocity of symmetric interfacial swimmers**. *Phys Rev Fluids* 2021, **6**, 104006, https://doi.org/10.1103/PhysRevFluids.6.104006.
The authors studied the effect of Marangoni flow on the symmetry breaking and swimming velocity of Marangoni surfers considering different limits of Peclet and Reynolds number.

155. Lauga E, Davis AMJ: **Viscous Marangoni propulsion**. *J Fluid Mech* 2012, **705**:120–133, https://doi.org/10.1017/jfm.2011.484.

156. Würger A: **Thermally driven Marangoni surfers**. *J Fluid Mech* 2014, **752**:589–601, https://doi.org/10.1017/jfm.2014.349.

157. Masoud H, Stone HA: **A reciprocal theorem for Marangoni propulsion**. *J Fluid Mech* 2014, **741**:R4, https://doi.org/10.1017/jfm.2014.8.

158. Vandadi V, Kang SJ, Masoud H: **Reverse Marangoni surfing**. *J Fluid Mech* 2017, **811**:612–621, https://doi.org/10.1017/jfm.2016.695.

159. ** Han K, Kokot G, Das S, Winkler RG, Gompper G, Snezhko A: **Reconfigurable structure and tunable transport in synchronized active spinner materials**. *Sci Adv* 2020, **6**, https://doi.org/10.1126/sciadv.aaz8535. eaaz8535, https://www.science.org/doi/10.1126/sciadv.aaz8535.
Using rotating magnetic field, the authors guide self-assembly of ferromagnetic colloids trapped at water–air interface into chain spinners. The chains can spin synchronously and generate strong hydrodynamic flows at the interface.

160. * Fei W, Tzelios PM, Bishop KJM: **Magneto-capillary particle dynamics at curved interfaces: time-varying fields and drop mixing**. *Langmuir* 2020, **36**, https://doi.org/10.1021/acs.langmuir.9b03119. acs.langmuir.9b03119, https://pubs.acs.org/doi/10.1021/acs.langmuir.9b03119.
Using time-varying magnetic field, the authors can guide the motion of magnetic Janus particles at oil droplets in circular orbits or along zigzag paths.

161. * Piñan Basualdo FN, Bolopion A, Gauthier M, Lambert P: **A microrobotic platform actuated by thermocapillary flows for manipulation at the air-water interface**. *Sci Robot* 2021, **6**, https://doi.org/10.1126/scirobotics.abd3557. eabd3557, https://www.science.org/doi/10.1126/scirobotics.abd3557.
Using separate lasers to induce thermocapillary flow around the objects, the authors managed to precisely control the motion of microrobots at interfaces.

162. Grosjean G, Hubert M, Vandewalle N: **Magnetocapillary self-assemblies: locomotion and micromanipulation along a liquid interface**. *Adv Colloid Interface Sci* 2018, **255**:84–93, https://doi.org/10.1016/j.cis.2017.07.019. https://linkinghub.elsevier.com/retrieve/pii/S0001868617300167.

163. Golosovsky M, Saado Y, Davidov D: **Self-assembly of floating magnetic particles into ordered structures: a promising route for the fabrication of tunable photonic band gap materials**. *Appl Phys Lett* 1999, **75**:4168–4170, https://doi.org/10.1063/1.125571. http://aip.scitation.org/doi/10.1063/1.125571.

164. Grzybowski BA, Stone HA, Whitesides GM: **Dynamic self-assembly of magnetized, millimetre-sized objects rotating at a liquid–air interface**. *Nature* 2000, **405**:1033–1036, https://doi.org/10.1038/35016528. http://www.nature.com/articles/35016528.

165. Grzybowski BA, Stone HA, Whitesides GM: **Dynamics of self assembly of magnetized disks rotating at the liquid–air interface**. *Proc Natl Acad Sci USA* 2002, **99**:4147–4151, https://doi.org/10.1073/pnas.062036699. https://pnas.org/doi/full/10.1073/pnas.062036699.

166. He Y, Wang L, Yang K, Wang X, Rong W, Sun L: **Cooperative self-assembled magnetic micropaddles at liquid surfaces**. *ACS Appl Mater Interfaces* 2021, **13**:46180–46191, https://doi.org/10.1021/acsami.1c13551. https://pubs.acs.org/doi/10.1021/acsami.1c13551.
Using rotating magnetic field and precessing magnetic field, the authors achieved the self-assembled chainlike micropaddles and their micro-manipulation at fluid interface.

167. Snezhko A, Aranson IS, Kwok W-K: **Surface wave assisted self-assembly of multidomain magnetic structures**. *Phys Rev Lett* 2006, **96**, 078701, https://doi.org/10.1103/PhysRevLett.96.078701. https://link.aps.org/doi/10.1103/PhysRevLett.96.078701.

168. Belkin M, Snezhko A, Aranson IS, Kwok W-K: **Driven magnetic particles on a fluid surface: pattern assisted surface flows**. *Phys Rev Lett* 2007, **99**, 158301, https://doi.org/10.1103/PhysRevLett.99.158301.

169. Snezhko A, Aranson IS: **Magnetic manipulation of self-assembled colloidal asters**. *Nat Mater* 2011, **10**:698–703, https://doi.org/10.1038/nmat3083. http://www.nature.com/articles/nmat3083.

170. Martínez-Pedrero F, González-Banciella A, Camino A, Mateos-Maroto A, Ortega F, Rubio RG, Pagonabarraga I, Calero C: **Static and dynamic self-assembly of pearl-like-chains of magnetic colloids confined at fluid interfaces**. *Small* 2021, **17**, 2101188, https://doi.org/10.1002/smll.202101188. https://onlinelibrary.wiley.com/doi/10.1002/smll.202101188.

171. * Fei W, Driscoll MM, Chaikin PM, Bishop KJM: **Magneto-capillary dynamics of amphiphilic Janus particles at curved liquid interfaces**. *Soft Matter* 2018, **14**:4661–4665, https://doi.org/10.1039/C8SM00518D. http://xlink.rsc.org/?DOI=C8SM00518D.
The magnetic Janus particles can translate under a static homogeneous magnetic field at the surface of droplet. The authors proposed a mechanism was proposed that couples the capillary torque and magnetic torque.

172. * Barbot A, Tan H, Power M, Seichepine F, Yang G-Z: **Floating magnetic microrobots for fiber functionalization**. *Sci Robot* 2019, **4**, eaax8336, https://doi.org/10.1126/scirobotics.aax8336.
The authors designed a floating microrobot pair that can grasp, align, position and release floating objects by simply changing the distance between two microrobots.

173. ** Dietrich K, Volpe G, Sulaiman MN, Renggli D, Buttinoni I, Isa L: **Active atoms and interstitials in two-dimensional colloidal crystals**. *Phys Rev Lett* 2018, **120**, 268004, https://doi.org/10.1103/PhysRevLett.120.268004. https://link.aps.org/doi/10.1103/PhysRevLett.120.268004.
The authors observed two behaviors of self-propelled Janus particle in a two-dimensional colloidal crystal. The active behaviors are undertood through electrostatic coupling between active colloids and passive colloidal monolayer.

174. Gouiller C, Ybert C, Cottin-Bizonne C, Raynal F, Bourgoin M, Volk R: **Two-dimensional numerical model of Marangoni surfers: from single swimmer to crystallization**. *Phys Rev* 2021, **104**, 064608, https://doi.org/10.1103/PhysRevE.104.064608. https://link.aps.org/doi/10.1103/PhysRevE.104.064608.

175. * Gouiller C, Raynal F, Maquet L, Bourgoin M, Cottin-Bizonne C, Volk R, Ybert C: **Mixing and unmixing induced by active camphor particles**. *Phys Rev Fluids* 2021, **6**, 014501, https://doi.org/10.1103/PhysRevFluids.6.014501. https://link.aps.org/doi/10.1103/PhysRevFluids.6.014501.
The authors observed a "turbulentlike" concentration spectra at the interfaces with presence of campher disks. The concentration field includes densely seeded regions and depleted regions.

176. Vialetto J, Anyfantakis M: **Exploiting additives for directing the adsorption and organization of colloid particles at fluid interfaces**. *Langmuir* 2021, **37**:9302–9335, https://doi.org/10.1021/acs.langmuir.1c01029. https://pubs.acs.org/doi/10.1021/acs.langmuir.1c01029.

177. Huang M, Hu W, Yang S, Liu Q-X, Zhang HP: **Circular swimming motility and disordered hyperuniform state in an algae system**. *Proc Natl Acad Sci USA* 2021, **118**, e2100493118, https://doi.org/10.1073/pnas.2100493118. https://pnas.org/doi/full/10.1073/pnas.2100493118.

178. Menath J, Eatson J, Brilmayer R, Andrieu-Brunsen A, Buzza DMA, Vogel N: **Defined core–shell particles as the key to complex interfacial self-assembly**. *Proc Natl Acad Sci USA* 2021, **118**, e2113394118, https://doi.org/10.1073/pnas.2113394118. https://pnas.org/doi/full/10.1073/pnas.2113394118.

179. Vialetto J, Camerin F, Grillo F, Ramakrishna SN, Rovigatti L, Zaccarelli E, Isa L: **Effect of internal architecture on the assembly of soft particles at fluid interfaces**. *ACS Nano* 2021, **15**:13105–13117, https://doi.org/10.1021/acsnano.1c02486. https://pubs.acs.org/doi/10.1021/acsnano.1c02486.

180. Wang L, Simmchen J: **Review: interactions of active colloids with passive tracers**. *Condens Matter* 2019, **4**:78, https://doi.org/10.3390/condmat4030078. https://www.mdpi.com/2410-3896/4/3/78.

181. * Martínez-Pedrero F, Ortega F, Rubio RG, Calero C: **Collective transport of magnetic microparticles at a fluid interface through dynamic self-assembled lattices**. *Adv Funct Mater* 2020, **30**, 2002206, https://doi.org/10.1002/adfm.202002206. https://onlinelibrary.wiley.com/doi/10.1002/adfm.202002206.
The authors managed to control the behaviors of different-sized magnetic particles by tuning the strength and orientation of the applied field. Their magnetic dipole interactions induce collective behaviors.

182. Pesic J, Terdik JZ, Xu X, Tian Y, Lopez A, Rice SA, Dinner AR, Scherer NF: **Structural responses of quasi-two-dimensional colloidal fluids to excitations elicited by nonequilibrium perturbations**. *Phys Rev* 2012, **86**, 031403, https://doi.org/10.1103/PhysRevE.86.031403. https://link.aps.org/doi/10.1103/PhysRevE.86.031403.

183. Weeber R, Harting J: **Hydrodynamic interactions in active colloidal crystal microrheology**. *Phys Rev* 2012, **86**, 057302, https://doi.org/10.1103/PhysRevE.86.057302. https://link.aps.org/doi/10.1103/PhysRevE.86.057302.

184. Masoud H, Shelley MJ: **Collective surfing of chemically active particles**. *Phys Rev Lett* 2014, **112**, 128304, https://doi.org/10.1103/PhysRevLett.112.128304. https://link.aps.org/doi/10.1103/PhysRevLett.112.128304.

185. Soh S, Bishop KJM, Grzybowski BA: **Dynamic self-assembly in ensembles of camphor boats**. *J Phys Chem B* 2008, **112**:10848–10853, https://doi.org/10.1021/jp7111457. https://pubs.acs.org/doi/10.1021/jp7111457.

186. Pototsky A, Thiele U, Stark H: **Stability of liquid films covered by a carpet of self-propelled surfactant particles**. *Phys Rev* 2014, **90**, 030401, https://doi.org/10.1103/PhysRevE.90.030401. https://link.aps.org/doi/10.1103/PhysRevE.90.030401.

187. Domínguez A, Malgaretti P, Popescu MN, Dietrich S: **Collective dynamics of chemically active particles trapped at a fluid interface**. *Soft Matter* 2016, **12**:8398–8406, https://doi.org/10.1039/C6SM01468B. http://xlink.rsc.org/?DOI=C6SM01468B.

188. Domínguez A, Popescu MN: **Phase coexistence in a monolayer of active particles induced by Marangoni flows**. *Soft Matter* 2018, **14**:8017–8029, https://doi.org/10.1039/C8SM00688A. http://xlink.rsc.org/?DOI=C8SM00688A.

189. Hirose Y, Yasugahira Y, Okamoto M, Koyano Y, Kitahata H, Nagayama M, Sumino Y: **Two floating camphor particles interacting through the lateral capillary force**. *J Phys Soc Jpn* 2020, **89**, 074004, https://doi.org/10.7566/JPSJ.89.074004. https://journals.jps.jp/doi/10.7566/JPSJ.89.074004.

190. Nakata S, Doi Y, Kitahata H: **Synchronized sailing of two camphor boats in polygonal chambers**. *J Phys Chem B* 2005, **109**:1798–1802, https://doi.org/10.1021/jp0480605. https://pubs.acs.org/doi/10.1021/jp0480605.

191. Morohashi H, Imai M, Toyota T: **Construction of a chemical motor-movable frame assembly based on camphor grains using water-floating 3D-printed models**. *Chem Phys Lett* 2019, **721**:104–110, https://doi.org/10.1016/j.cplett.2019.02.034. https://linkinghub.elsevier.com/retrieve/pii/S0009261419301538.

192. Nishimori H, Suematsu NJ, Nakata S: **Collective behavior of camphor floats migrating on the water surface**. *J Phys Soc Jpn* 2017, **86**, 101012, https://doi.org/10.7566/JPSJ.86.101012. http://journals.jps.jp/doi/10.7566/JPSJ.86.101012.

193. Ikura YS, Heisler E, Awazu A, Nishimori H, Nakata S: **Collective motion of symmetric camphor papers in an annular water channel**. *Phys Rev* 2013, **88**, 012911, https://doi.org/10.1103/PhysRevE.88.012911. https://link.aps.org/doi/10.1103/PhysRevE.88.012911.

194. Schulz O, Markus M: **Velocity distributions of camphor particle ensembles**. *J Phys Chem B* 2007, **111**:8175–8178, https://doi.org/10.1021/jp072677f. https://pubs.acs.org/doi/10.1021/jp072677f.

195. Singh DP, Domínguez A, Choudhury U, Kottapalli SN, ** Popescu MN, Dietrich S, Fischer P: **Interface-mediated spontaneous symmetry breaking and mutual communication between drops containing chemically active particles**. *Nat Commun* 2020, **11**:2210, https://doi.org/10.1038/s41467-020-15713-y. http://www.nature.com/articles/s41467-020-15713-y.
The authors observed that the homogeneous particles inside the sessile droplet can self-organize into two symmetric vortices due to the Marangoni effect. The alignment of the flow in the droplet is coupled with its neighboring drop through mutual chemical communication.

196. Bourgoin M, Kervil R, Cottin-Bizonne C, Raynal F, Volk R, Ybert C: **Kolmogorovian active turbulence of a sparse assembly of interacting Marangoni surfers**. *Phys Rev X* 2020, **10**, 021065, https://doi.org/10.1103/PhysRevX.10.021065.

197. Liebchen B, Marenduzzo D, Cates ME: **Phoretic interactions generically induce dynamic clusters and wave patterns in active colloids**. *Phys Rev Lett* 2017, **118**, 268001, https://doi.org/10.1103/PhysRevLett.118.268001. http://link.aps.org/doi/10.1103/PhysRevLett.118.268001.

198. Wioland H, Lushi E, Goldstein RE: **Directed collective motion of bacteria under channel confinement**. *New J Phys* 2016, **18**, 075002, https://doi.org/10.1088/1367-2630/18/7/075002. https://iopscience.iop.org/article/10.1088/1367-2630/18/7/075002.

199. Zaki H, Lushi E, Severi KE: **Larval zebrafish exhibit collective circulation in confined spaces**. *Front Phys* 2021, **9**, 678600, https://doi.org/10.3389/fphy.2021.678600. https://www.frontiersin.org/articles/10.3389/fphy.2021.678600/full.

200. Lushi E, Wioland H, Goldstein RE: **Fluid flows created by swimming bacteria drive self-organization in confined suspensions**. *Proc Natl Acad Sci USA* 2014, **111**:9733–9738, https://doi.org/10.1073/pnas.1405698111. https://pnas.org/doi/full/10.1073/pnas.1405698111.

201. Pierce C, Wijesinghe H, Mumper E, Lower B, Lower S, Sooryakumar R: **Hydrodynamic interactions, hidden order, and emergent collective behavior in an active bacterial suspension**. *Phys Rev Lett* 2018, **121**, 188001, https://doi.org/10.1103/PhysRevLett.121.188001. https://link.aps.org/doi/10.1103/PhysRevLett.121.188001.

202. Théry A, Le Nagard L, Ono-dit Biot J-C, Fradin C, Dalnoki- * Veress K, Lauga E: **Self-organisation and convection of confined magnetotactic bacteria**. *Sci Rep* 2020, **10**, 13578, https://doi.org/10.1038/s41598-020-70270-0. https://www.nature.com/articles/s41598-020-70270-0.
The authors studied behaviors of magnetotactic bacteria reoriented by a perpendicular magnetic field near a solid wall. Bacteria can self-organize into vortex structure near the wall.

203. Crossley S, Faria J, Shen M, Resasco DE: **Solid nanoparticles that catalyze biofuel upgrade reactions at the water/oil interface**. *Science* 2010, **327**:68–72, https://doi.org/10.1126/science.1180769. https://www.science.org/doi/10.1126/science.1180769.

204. Vaccari L, Molaei M, Leheny RL, Stebe KJ: **Cargo carrying * bacteria at interfaces**. *Soft Matter* 2018, **14**:5643–5653, https://doi.org/10.1039/C8SM00481A. http://xlink.rsc.org/?DOI=C8SM00481A.
Bacteria can adhere to the passive colloids at the interfaces and drive them along persistent, and curly trajectories.

205. Wu X-L, Libchaber A: **Particle diffusion in a quasi-two-dimensional bacterial bath**. *Phys Rev Lett* 2000, **84**:3017–3020, https://doi.org/10.1103/PhysRevLett.84.3017. https://link.aps.org/doi/10.1103/PhysRevLett.84.3017.

206. Mathijssen AJTM, Pushkin DO, Yeomans JM: **Tracer trajectories and displacement due to a micro-swimmer near a surface**. *J Fluid Mech* 2015, **773**:498–519, https://doi.org/10.1017/jfm.2015.269.

207. Pushkin DO, Shum H, Yeomans JM: **Fluid transport by individual microswimmers**. *J Fluid Mech* 2013, **726**:5–25, https://doi.org/10.1017/jfm.2013.208.

208. Kanazawa K, Sano TG, Cairoli A, Baule A: **Loopy Lévy flights ** enhance tracer diffusion in active suspensions**. *Nature* 2020, **579**:364–367, https://doi.org/10.1038/s41586-020-2086-2. http://www.nature.com/articles/s41586-020-2086-2.
The authors developed a theoretical framework to model the hydrodynamic interactions between the tracer and the active swimmers, which showed that the tracer follows a non-Markovian coloured Poisson process that accounts for all empirical observations.

209. Gordon VD, Wang L: **Bacterial mechanosensing: the force will be with you, always**. *J Cell Sci* 2019, **132**, https://doi.org/10.1242/jcs.227694. jcs227694, https://journals.biologists.com/jcs/article/132/7/jcs227694/57420/Bacterial-mechanosensing-the-force-will-be-with.